FINNISH ROAD ADMINISTRATION

Leena Korkiala-Tanttu, Rainer Laaksonen and Jouko Törnqvist

Reinforcement of the edge of a steep-sloped pavement

HVS-Nordic Heavy Vehicle Simulator test structures

Finnra Reports 38/2003

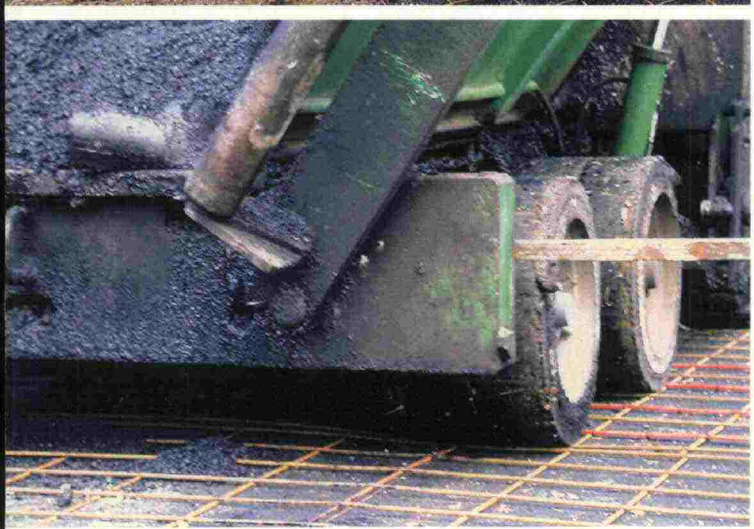

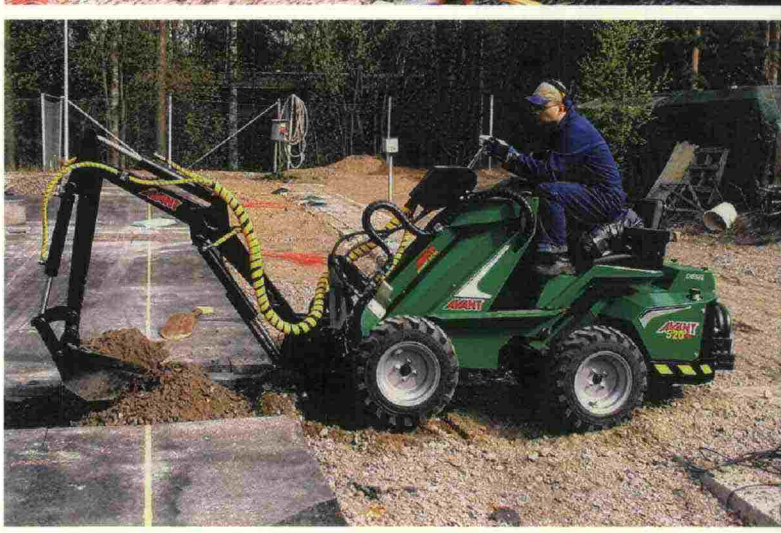

Leena Korkiala-Tanttu, Rainer Laaksonen and Jouko Törnqvist

Reinforcement of the edge of a steep-sloped pavement

HVS-Nordic Heavy Vehicle Simulator test structures

Finnra Reports 38/2003

Finnish Road Administration
Helsinki 2003

Pictures of the cover: Building and decommission of the test structure.

ISSN 1457-9871
ISBN 951-803-107-x
TIEH 3200825E

Network publication pdf (www.tiehallinto.fi/julkaisut)
ISSN 1459-1553
ISBN 951-803-108-8
TIEH 3200825E-v

Multiprint Oy
Vaasa 2003

Publication sold by/available at:
Finnish Road Administration, publication sales
Telefax +358 (0) 204 22 2652
E-mail: julkaisumyynti@tiehallinto.fi

Finnish Road Administration
Opastinsilta 12 A
P.O.Box 33
FIN-00521 HELSINKI
Tel. exchange +358 (0) 204 22 150

Leena Korkiala-Tanttu, Rainer Laaksonen, Jouko Törnqvist; Reinforcement of the edge of a steep-sloped pavement. HVS-Nordic Heavy Vehicle Simulator test structures.
Helsinki 2003. Finnish Road Administration. Finnra Reports 38/2003. 46 p. + app. 24 p.
ISSN 1457-9871, ISBN 951-803-107-x, TIEH 3200825E.

Keywords: low volume road, rehabilitation, accelerated pavement test, rutting, permanent deformation, steel grid, geotextile
Classification: 32, 70

SUMMARY

This study is part of the research project Economical Maintenance of Low-volume Roads. It focuses on the behaviour of roads with low bearing capacity by studying the effect of rehabilitation on the performance of a steep-sloped pavement structure. The study was commissioned by Finnish Road Administration Finnra. The research was in part financed by steel grid manufacturers Pintos Oy and Tammet Oy and geotextile manufacturer Polyfelt Ges.m.b.H.

The test structures loaded in the Low-volume road project and subsequently rehabilitated were tested with the HVS Nordic heavy vehicle simulator. The rehabilitation included levelling the ruts and installing various reinforcements, as well as spreading a new surface layer. Six structures were being tested: two unreinforced reference structures, one structure reinforced with fibreglass and three reinforced with steel grid. Two types of steel grid were used: B500H - 5/6 - 200/150 and B500H - 5/8 - 200/150. That is, the grids differed only in the thickness of the transverse wire (6 mm and 8 mm). The structures were loaded using a similar loading programme as for the Low-volume road project. The loading variables in the tests were axle load and water table level. The test wheel was a Super Single tyre. The load varied between 30 kN and 50 kN and the water table level was elevated gradually from the top of the subgrade to the middle of the base course during the heaviest loading phase.

The aim of the research was to study what effect the reinforcement grid used in the rehabilitation of rutted structures has on decelerating rutting in structures with low bearing capacity edges. The second aim was to find out whether different reinforcement grids differed in decelerating rutting.

The test structures were designed to correspond to the structure of low-volume roads and were built in the concrete basin at VTT's facilities in Otaniemi. The loaded structures were rehabilitated by levelling the ruts, installing the reinforcements and spreading a new surface layer. The overall thickness of the pavement before rehabilitation was 650 mm. 400 mm of the pavement consisted of base course crushed rock and 200 mm of subbase gravel and the subgrade was clayey silt. The thickness of the levelling mix and the new surface layer on the loading area was 139–188 mm, with the thickest new surface layer coinciding with the previous steep-sloped structure. The three test structures in the Low-volume road project were each divided in two, yielding three pairs of structures. The first pair of structures (the former structure with no slope), as well as the third pair of structures (the former structure with the 1:1.5 slope), contained both an unreinforced reference structure and B500H - 5/6 - 200/150 steel grid. The second pair of structures contained B500H - 5/8 - 200/150 steel grid and fibreglass reinforcement.

The reinforcements were anchored outside the basin. The anchoring aimed at simulating a situation in which the reinforcement extends across the entire road and it is also loaded by the weight of the surface layer on the other lane. The fibreglass reinforcement was installed according to the

manufacturer's instructions by gluing it with bitumen emulsion. The steel grids were instrumented with strain gauges and an accelerometer was installed on top of the surface layer for measuring surface layer deflection.

The rehabilitation was successful. After the heavy vehicle simulator was moved to the site, the side slope was dug open. All structures had 1:1.5 side slopes. The states of the structures differed after the rehabilitation because the structure that had become the most rutted in the first phase of tests had the thickest new surface layer. However, falling weight deflectometer measurements before and after the test did not show significant differences between the different structures. The different reinforcements did not seem to have a significant effect on the bearing capacity values determined with the falling weight deflectometer. The structure pairs with greater differences in rut depth, however, also yielded greater differences in bearing capacity.

The rutting and distress of the structures were monitored during the test. However, no distress was perceived at the end of the test, so the comparisons are only made for rutting. No differences were perceived in the performance of the different reinforcements.

The target rut depth for the tests was 15 mm. This, however, was achieved in none of the structures due to reasons associated with the schedule. Consequently, the service life analyses include extrapolations to the rut depth of 15 mm for different structures. The reinforced structure in pair 24 - 25 (former structure with no slope) rutted approximately 25–30% slower than the corresponding unreinforced structure, while the reinforced structure in pair 28 - 29 (former 1:1.5 slope) rutted 55–60% slower than the unreinforced structure. The rutting of the reinforced structures in pair 26 - 27 falls between these values. The deceleration of rutting in structures 24 - 25 corresponds to approximately 40 – 50% extension to service life. Correspondingly, the deceleration in structures 28 - 29 means approximately 130 – 190% longer service life. The great differences in structure performance can be explained not only by deformations already existing in the structures, but also by the fact that the thickness of the pavements differed approximately 30%. Other factors could include variation in how the surface layers adhered to each other and variation associated with the building.

The distribution of permanent deformations in the structures probably conforms to the pattern in the Low-volume road project, although the deformations remained noticeably smaller. The majority of deformations occurred in the base course.

The earth pressures for unbound layers showed a clear decrease thanks to the rehabilitation. Earth pressures were only monitored between different structure pairs because the location of the pressure cells varied within the pairs of structures, some being in the reinforced and some in unreinforced areas. In the gravel layer, the decrease was approximately 42 percent in structures 24 - 25, and in structures 28 - 29 approximately 58 percent. Deeper down in the subgrade clay the difference was also approximately 28 percent in structures 24 - 25 and, on average, 48 percent in structures 28 - 29. The values in structures 26 - 27 fall between these values.

When dismantling the structures, it was discovered that there were great differences in the adhesion between the old and new surface layer. Some structures, such as the fibreglass mesh glued with bitumen emulsion, adhered to the surface layer uniformly, while in structure 24 - 25, the new surface layer and the steel grid embedded in it had come completely apart. The surface layers had also come unstuck in the corresponding reference structure.

FOREWORD

This study 'Reinforcement of the edge of a steep-sloped pavement' is part of a research project to develop economical maintenance of low-volume roads. The study focuses on the performance of roads with low bearing capacity. In addition to funding from the Finnish Road Administration Finnra, the research was financed in part by steel grid manufacturers Pintos Oy and Tammet Oy and geotextile manufacturer Polyfelt Ges.m.b.H. The study was carried out by VTT Building and Transport according to the research plan and under the supervision of Finnra and the other financiers.

The aim of the study was to find out

- how the reinforcement grid used in resurfacing decelerates rutting on a narrow road with steep slopes, which was previously rutted by heavy vehicles; and
- are there differences in the performance of different reinforcement grids?

Planning meetings were held during the research project to discuss the testing arrangements with the steering group. Members of the steering group were informed of the progress and they commented on the report. The members of the steering group were:

Kari Lehtonen	Finnish Road Administration Finnra
Jussi Syrjynen	Tammet Oy
Jouko Varttinen	Pintos Oy
Rainer Lugmayr	Polyfelt Ges.m.b.H.

The research was carried out by VTT Building and Transport. Markku Tuhola, Jari Pihlajamäki, Jouko Törnqvist and Leena Korkiala-Tanttu were responsible for the preparation and planning of the research. Construction, instrumentation and loading the structures was carried out by Pekka Halonen and Janne Sikiö. Rainer Laaksonen was responsible for the laboratory tests. The laboratory tests for clay samples were conducted at the Department of Civil and Environmental Engineering of Helsinki University of Technology. Leena Korkiala-Tanttu, Pekka Halonen and Rainer Laaksonen were responsible for analysing the test data, collecting the results for the subtasks and writing the report.

Espoo, August 2003

VTT Building and Transport

Tiehallinto

Contents

1 INTRODUCTION

1.1 Background and objectives

This study 'Reinforcement of the edge of a steep-sloped pavement' is part of a research project to develop economical maintenance of low-volume roads. The project focuses on the performance of roads with low bearing capacity. These roads are characterised by extremely heavy single loads in relation to the bearing capacity, steep inside slopes, reduction in bearing capacity caused by thawing of frozen soil, as well as heterogeneity in structural engineering due to the way the road network has been built over time.

The research project 'Reinforcement of the edge of a steep-sloped pavement' studied the conventional ways of rehabilitating rutted road structures with low bearing capacity and their effect on rutting speed. The study sought to discover how effective different measures are and, thus, how economical they are from the point of view of those responsible for the maintenance of the road. The research helps to enhance the cost-effectiveness of maintenance and rehabilitation of low-volume roads and improve customer satisfaction.

The project studied the differences between reinforced and unreinforced structures. Several test structures were built in an identical way but using different reinforcement materials. This made it possible to directly compare the performance and effectiveness of different reinforcement materials in rehabilitated sites.

The study aimed at discovering the effect of the rehabilitation: how fast does a steep-sloped pavement become rutted after the rehabilitation in comparison to the same road subjected to the same load before the rehabilitation? The study also aimed at discovering how much different methods of reinforcing decelerate rutting. This information is necessary when assessing the differences in the quality of rehabilitation solutions offered by subcontractors.

1.2 Test structures

VTT has test basins in Otaniemi, Espoo, for conducting load tests with the Heavy Vehicle Simulator (HVS Nordic). The test site has two basins: one made from concrete and one blasted in rock. The tests in this study were carried out in the concrete basin on the test structures constructed for the Low-volume roads study. The structures were repaired to correspond to rehabilitated steep-sloped road constructions.

More detailed descriptions of the test basin, building of the constructions tested in the Low-volume roads project and their instrumentation, as well as analysis of the results, can be found in the HVS report '*Effect of steepness of side slope on rutting*' /Korkiala-Tanttu *et al.* 2002a/.

1.3 Load with Heavy Vehicle Simulator (HVS)

The Heavy Vehicle Simulator (HVS) is 23 m long, 3.7 m wide, 4.2 m high and its total mass is 46 metric tons (Figure 1.1). The maximum width of HVS's loading area is 1.5 m. The total length of the loading area is eight metres, of which six metres can be used with even wheel load and speed. At either end of the loading area, a distance of one metre is necessary for accelerating and braking the wheel, and, in one-way application of load, for lowering and lifting the wheel to and from the surface. The speed of the wheel can be adjusted from 1 to 15 km/h. However, in long-term loading, the maximum speed is 12 km/h. Any distribution with 50 mm lateral adjustments can be selected as the lateral movement of the test wheel. The load can be applied either one-way or in both directions.

Figure 1.1. The Heavy Vehicle Simulator (HVS).

The maximum load achieved with the simulator is 110 kN and the minimum 25 to 30 kN. The load can be applied on the structure via either a single lorry tyre or twin tyre. In addition, the load can be given a dynamic extra load to simulate the additional stress caused by the unevenness of the road. With the simulator, it is in theory possible to achieve 25,000 load repetitions in 24 hours (bi-directional load).

The simulator includes a heating/cooling unit for keeping the road structure to be tested at the desired temperature. Moving the equipment requires dismantling the insulation box, and in major moves, also detaching the test wheel.

2 BUILDING AND INSTRUMENTATION

2.1 Tested structures

Three structures, 8 m in length, that had become rutted and otherwise damaged in the tests for the Low-volume roads project were used as the base for the tested structures in this study. The structures were one with no slope, one with a gentle slope (1:3) and one with a steep slope (1:1.5). The previous tests studied the effect of slope steepness and position on rutting. Due to differences in the cross-sections, the structures had clearly rutted differently. The deepest ruts were approximately 55 mm (steep slope) and the shallowest approximately 28 mm (no slope).

For this study, the 8-metre long test structures were divided into two 4-metre strips each, which could be directly compared. In order to obtain comparable results between the different structures, two identical pairs of structures were tested, each with steel grid 1 and an unreinforced reference structure. The numbers of these structures were 24 and 25, and 28 and 29. The middle structures were reinforced with another type of steel grid and fibreglass reinforcement. The structures were repaired by filling in the ruts and then spreading a new asphalt layer over the entire structure. The reinforcements used, the positions of the structures – also in relation to the old structures – and their numbering are presented in Figure 2.1 and Table 2.1.

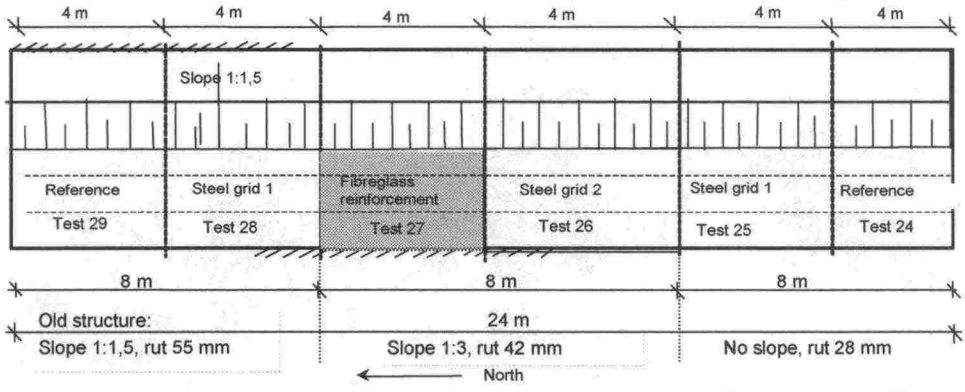

Figure 2.1. Test structures and their state before rehabilitation.

Table 2.1. Test structure and their state before rehabilitation

Structure	LV-structure	Rut depth before, mm	Reinforcement
24	No slope	28 mm	Reference with no reinforcement
25			Steel grid 1 (BH500 - 6/5 - 150/200)
26	Gentle slope 1:3	42 mm	Steel grid 2 (BH500 - 8/5 - 150/200)
27			Fibreglass reinforcement
28	Steep slope 1:1,5	55 mm	Steel grid 1 (BH500 - 6/5 - 150/200)
29			Reference with no reinforcement

The standard cross-section of the test structures is presented in Figure 2.2. After the first phase tests were completed, the structures, which had rutted during the loading, remained outside unprotected over the winter 2001–2002. Towards the end of the previous testing phase, the tops of the topmost Emu-Coil sensors had been excavated and levelled. Furthermore, the bearing capacity of the structures after the tests had been determined with Loadman measurements. The structures had visibly rutted in the first phase of the study and cracks could be observed. The cracks were mainly short and narrow. Only the inside edge of the rut in the structure with the steep slope (structure 28–29) showed a crack for the entire length of the rut.

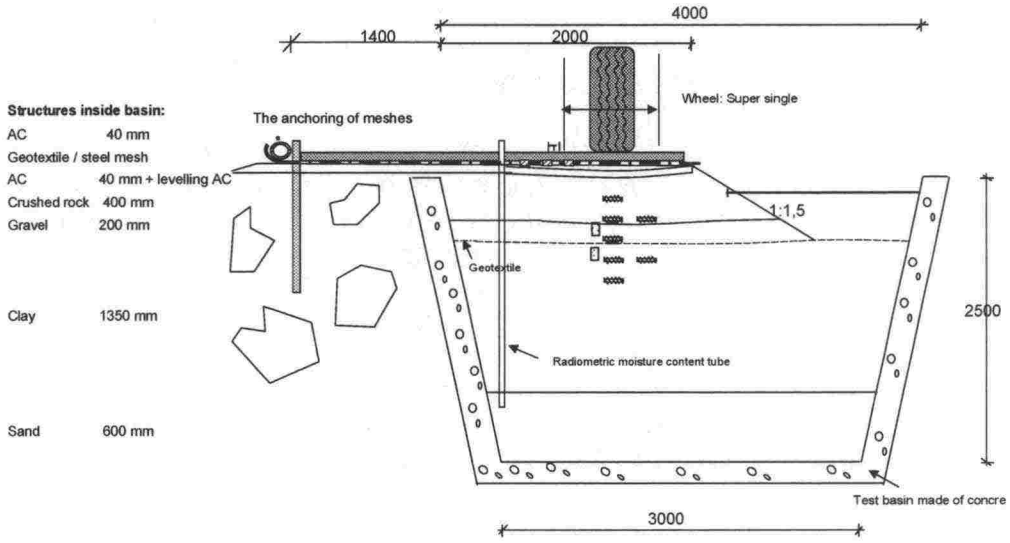

Figure 2.2. Cross-section of the test structure with the steep slope.

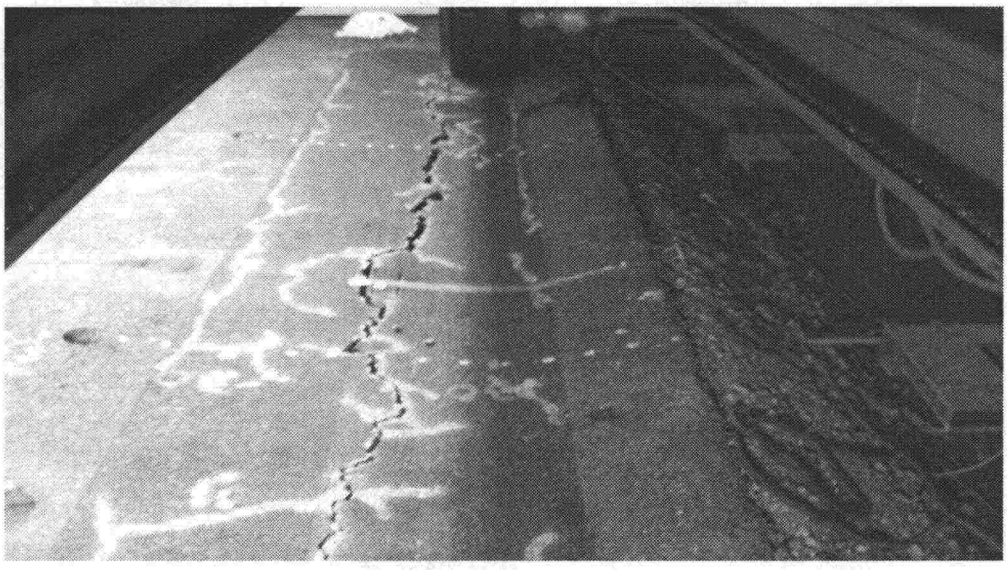

Figure 2.3. The test structure with the steep slope before repairing

The structures were rehabilitated by first levelling out the rut with levelling mix and then installing the reinforcements on the levelled surface. A 40 mm layer of asphalt was finally spread over the reinforcements. A steep (1:1.5)

slope was dug alongside the test structure after the heavy vehicle simulator was moved to the site, but before the loading began.

2.2 Pavements

The low-volume pavement was designed to have a bearing capacity corresponding to the structure of low-volume roads. A more detailed description of the materials, building and instrumentation is presented in the report '*Effect of steepness of side slope on rutting*' /Korkiala-Tanttu *et al.* 2002a/. Below is only a brief description of the properties of each pavement layer.

The subgrade of the basin consisted of a layer of lean clay, the total thickness of which in the beginning of the test was 1,350 mm. An application class 3 filter cloth was placed on top of the clay layer and a 3-metre wide bi-component geotextile at the ends of the basin. The bi-component geotextiles were installed in order to test their performance, which is discussed in a separate report /Korkiala-Tanttu *et al.* 2002b/.

The lowest layer of the unbound pavement (subbase) consisted of a 200 mm layer of compacted gravel (sandy gravel) and the upper layer (base course) of 400 mm of crushed rock ('Teisko crushed rock'). The bound pavement consisted of 40 mm asphalt (AB16/100) with grain size of 0–16 mm, and bitumen B70/100.

The construction work for the first phase was carried out in autumn 2000 and the test structure was then protected for the winter by insulating it. The actual testing took place in summer and autumn 2001. The structure remained outside unprotected over the winter 2001–2002.

2.3 Reinforcements

One aim of building the test structures was to determine the effect of different reinforcements on the rutting speed of a structure with low bearing capacity. The research team and the steel grid manufacturers agreed to test steel grids with identical grid openings. It was agreed that the primary steel grid to be tested would be the most popular type today (6/5 - 150/200), in which the transverse wire was 6 mm and the longitudinal wire 5 mm. Transverse wires were spaced at 150 mm and the longitudinal at 200 mm intervals (steel grid 1). The second grid selected for the tests (steel grid 2) was otherwise identical, but the diameter of its transverse wire was 8 mm. The steel grade in the grids was BH500. The length of the grids was 2 m and width 3.5 m. Two grids were installed in the longitudinal direction, joined by a butt seam, in order to achieve the structure's length of 4 m. The steel grids were installed with the longitudinal wire on the underside. The reinforcements were anchored around a 36 mm diameter steel tube outside the basin (Figure 2.2). The purpose of the anchoring was to simulate the anchoring effect caused by the weight of the other lane when a full-width steel grid is installed on a 7 m wide normal road. One edge of the steel grid was bent at the factory to fit the steel tube. Finally a 40 mm layer of asphalt was spread over the reinforcements. The steel grids were instrumented with strain gauges, which measured stress forming in the transverse steel wire.

The fibreglass reinforcement chosen was Polyfelt PGM-G100/100 supplied by Polyfelt Ges.m.b.H. It is designed for road construction and its tensile strength in both directions is 100 kN/m. This strength corresponds roughly to the strength of the steel grids. The fibreglass reinforcement was glued on both sides with bitumen emulsion according to the manufacturer's instructions. The fibreglass reinforcement was also anchored to the steel pipe by winding the reinforcement tightly around the pipe and doubling the extra material for 400 mm. The reinforcement was kept tight during the spreading of the bitumen emulsion and the asphalt layer to avoid folds. Due to the structure of the fibreglass reinforcement, tensile strain gauges could not be installed at a reasonable cost.

2.4 Construction

Building the new test structures began in August 2002. The work began by levelling the surface of the test structure. Holes were patched and the ruts were levelled with levelling mix. The protective tubes of pore pressure and radiometric sensors were extended to enable measurement during the new tests. Reinforcements were installed on the top and anchored as shown in Figure 2.2. The fibreglass reinforcement was glued to the base and the new asphalt layer with bitumen emulsion according to the manufacturer's instructions. Finally a 40 mm layer of asphalt was spread over the reinforcements. The asphalt used was the same quality as the lower layer, that is, (AB 16/100) and the bitumen 70/100. The steel grids were tightened with lines from the side of the slope to achieve prestressing.

The asphalt was compacted in the normal way with a smooth roller. The asphalt was spread over approximately 3.8 m laterally. The quality of the work was monitored with levelling, as well as DOR and falling weight deflectometer measurements. The slope trench was filled up during the falling weight deflectometer measurements prior to the tests, except for structure 28–29. Finally, the layer was instrumented. The slopes were dug open structure by structure only after the heavy vehicle simulator had been moved on top of the test structure. It was necessary to fill the slope trench again before the HVS was moved off the structure. The structures were tested in pairs, the order being 28 and 29, 26 and 27, and finally, 24 and 25.

The purpose of the tests and measurements conducted during construction and before actual testing was to study those properties of test structure materials the changes in which were to be monitored during and after the testing. The tests also formed part of the quality control of the test structures. The quality control results of the construction phase are presented in Appendix 2.

2.5 Controlling the water table level and the loading programme

The test was organised mainly like the tests in the Low-volume roads project. Prior to actual testing the water table level was elevated to the bottom of the subbase (W2 = +15.95) for a few days. After this, it was lowered to the basic level during testing (W1 = +15.70, 50 mm below the surface of the subgrade). Falling weight deflectometer measurements were conducted during the higher level of ground water.

During the 50 kN load in the loading of each section, the ground water table was elevated to the top of the gravel layer (W2 +15.95), and also to the layer of crushed rock (W3 +16.15).The variation in the ground water level and the loads on each section are presented in Figure 2.3 and Table 2.2.

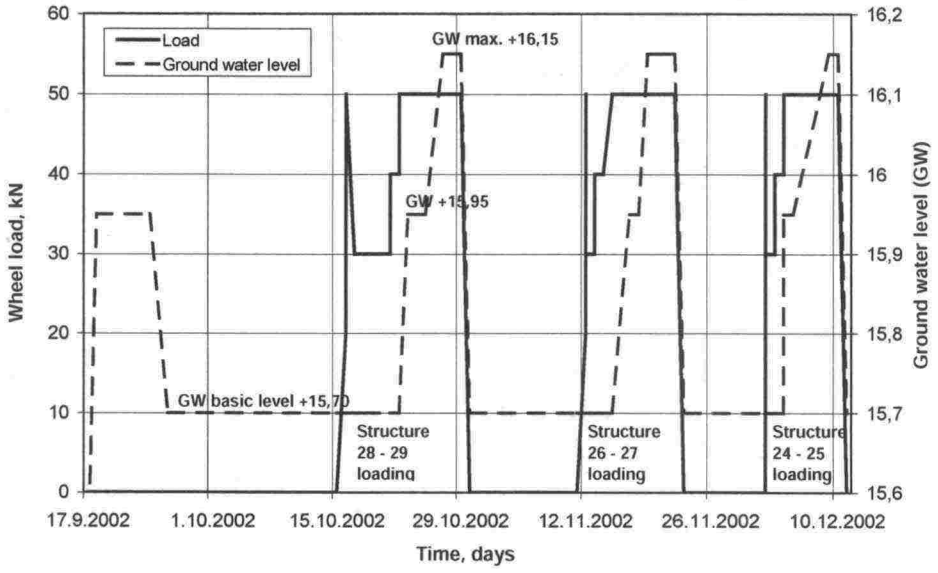

Figure 2.4. Ground water level and loading times of the different sections.

Table 2.2. Loading schedule (FWD = falling weight deflectometer).

Structure	Date	N	Load, kN	Ground water level	Notes
-	11.9.2002	-	-	+15.50	Elevating ground water level begins
-	18.9.2002	-	-	+15.95	Repairing ruts + FWD measurements
-	24.9.2002	-	-	+15.95	Spreading asphalt layer + FWD measurements
28–29	15.10.2002	-	-	+15.70	Initial measurements
	16.10.2002	560	30–50	+15.70	Preloading
	21.10.2002	8,900	30	+15.70	loading stage 1
	22.10.2002	17,300	40	+15.70	loading stage 2
	22.10.2002	24,400	50	+15.70	loading stage 3
	25.10.2002	28,300	50	+15.95	loading stage 4
	29.10.2002	38,900	50	+16.15	loading stage 5
26–27	11.11.2002	-	-	+15.70	Initial measurements
	12.11.2002	560	30–50	+15.70	Preloading
	13.11.2002	8,900	30	+15.70	loading stage 1
	14.11.2002	17,300	40	+15.70	loading stage 2
	15.11.2002	24,500	50	+15.70	loading stage 3
	18.11.2002	28,100	50	+15.95	loading stage 4
	21.11.2002	39,000	50	+16.15	loading stage 5
24–25	2.12.2002	-	-	+15.70	Initial measurements
	2.12.2002	560	30–50	+15.70	Preloading
	3.12.2002	8,900	30	+15.70	loading stage 1
	4.12.2002	17,300	40	+15.70	loading stage 2
	4.12.2002	24,500	50	+15.70	loading stage 3
	5.12.2002	28,200	50	+15.95	loading stage 4
	10.12.2002	39,000	50	+16.15	loading stage 5

All the structures were loaded according to the same loading programme (Table 2.2). The test wheel was a Super Single wheel and the tyre pressure on all wheel loads was 700 kPa. The loading distribution was the normal distribution based on studies of road structures. The width of the distribution was ± 300 mm from the centre. This loading distribution differed from the one used in the Low-volume roads study, which used three loading lines at 300 mm intervals, all loaded identically. The centrelines of the loads and instruments were located 700 mm from the edge of the slope, which also marked the edge of the asphalt layer. The structure responses were measured when the wheel load was on two positions: at the centre line and 300 mm left of the centre line (1000 mm from the edge of the asphalt layer).

2.6 Instrumentation

Instrumentation was used for measuring structural deformations, tensile strain in the reinforcements, earth pressure, and changes in moisture content and temperature, during both construction and testing. The instruments located in the pavements were installed in connection with constructing the pavements for the previous tests. It was not possible to monitor all previously installed instruments, or monitoring them was not deemed necessary for this study. For instance, the pore pressure transducers, which had been in the structures for two years, no longer worked.

New instruments installed during the construction phase included strain gauges in the steel grids and accelerometers measuring the deflection of the asphalt surface. Table 2.3 presents the types and numbers of instruments monitored during the testing. Detail drawings of the instrumentation of the various structures are in Appendix 1. Both atmospheric air and structure temperature was monitored during the tests in order to keep the test structure temperature constant (approximately + 10° C) during the tests.

Table 2.3. Instruments monitored in the study.

Measured quantity	Instrument	Number in different loading areas
Earth pressure	pressure cell	6 + 6 + 6
Temperature profile	thermocouple	1 + 1 + 1
Displacement	Emu-Coil	8 + 8 + 8
Density and volumetric water content	radiometric measuring tube	1 + 1 + 1
Atmospheric air temperature	temperature gauge	1
Asphalt temperature	copper constantan thermocouple	3 + 3 + 3
Deflection	accelerometer	2
Horizontal displacement in slope	LVDT displacement gauge (transfer from one structure to another)	2
Reinforcement tensile strain	strain gauge	12 + 12 + 12

3 LABORATORY TESTS

3.1 Laboratory tests for unbound materials

Materials

These tests concern the material properties which have not previously been studied in other phases of the study, that is, strength properties of the sandy gravel in the subbase and the deformation and strength properties of the clay representing the subgrade.

Clay

The index, deformation and strength properties of the clay were determined at the Laboratory of Soil Mechanics and Foundation Engineering at Helsinki University of Technology. The deformation properties were determined with a consolidation test and the strength properties with a triaxial test. According to the grain size analysis, the material was lean clay.

The deformation tests were carried out with a consolidation test in progressive steps, using ten loading steps (3.125–800 kPa). The sample for the consolidation test measured (diameter x height) 50 x 20 mm. The test also included an unloading – repeated loading phase. The results for the deformation tests are given in Table 3.1 and the load – deformation curve in Figure 3.1.

Table 3.1. Consolidation test. HVS steep slope, clay. Test results.

Density (g/cm^3)	Water content (%)	m_1 (kPa)	β_1 (-)	m_2 (kPa)	β_2 (-)
1.958	27.3	55.3	0.40	110	0.50

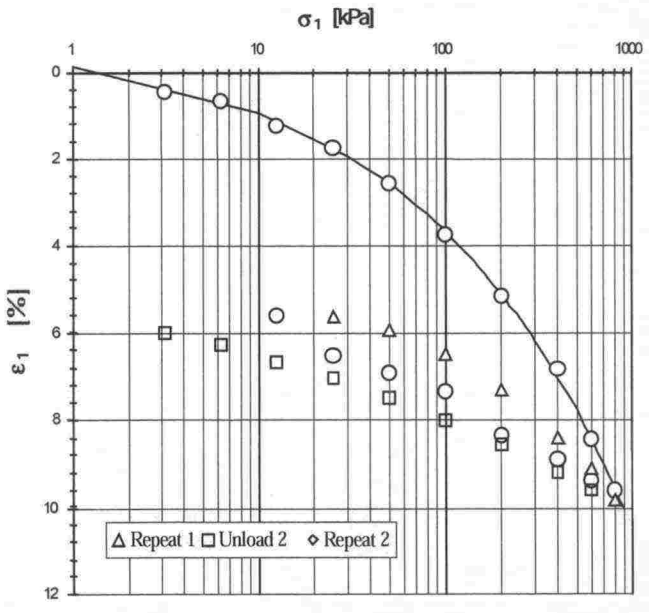

Figure 3.1. Consolidation test. Clay. Load-deformation curve.

The triaxial test for clay was carried out on four different confining pressures: 10, 20, 40 and 80 kPa. The anisotropically consolidated samples were sheared in undrained conditions. The size of the sample (diameter x height) was 50 x 100 mm. The shearing speed was 0.02 mm/min, or 1.2 mm/h. The degree of saturation of the samples at the shearing phase varied between 90–100%.

The stress paths of the triaxial tests are presented in Figure 3.2, which also shows a straight line used for calculating the strength parameters. The strength parameters determined from the results of the triaxial tests are presented in Table 3.2.

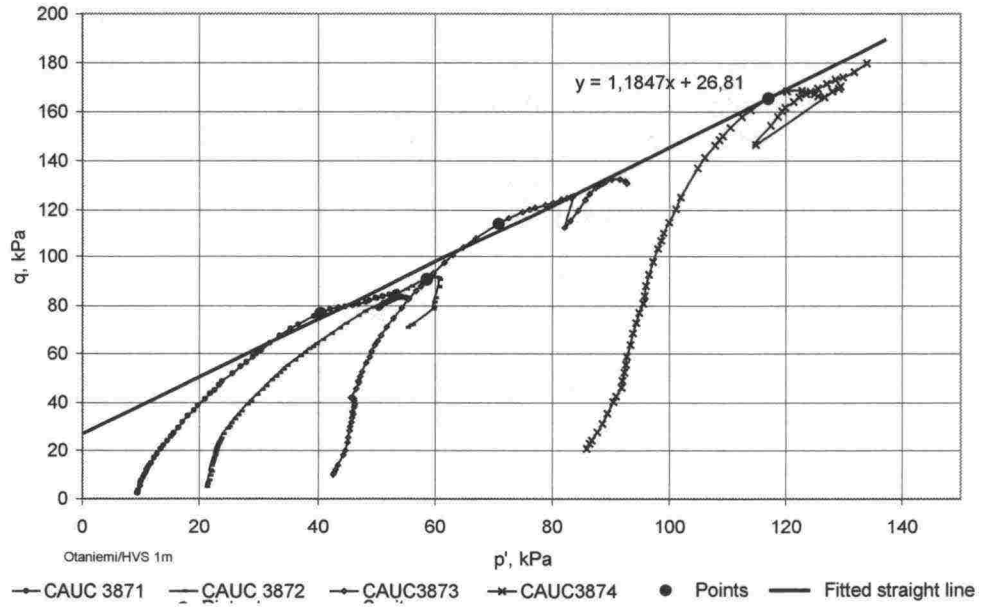

Figure 3.2. Triaxial test. Clay. Stress paths.

Table 3.2. Triaxial test. Clay. Strength parameters.

Density, average (g/cm3)	Water content, average (%)	Angle of friction	Cohesion
1.863	32.4	29.6	12.9

The triaxial tests were successful and it was possible to determine undrained strength parameters for the clay. The angle of friction determined fits well within the loose state values (27-30°) prescribed for clay in the foundation engineering guidelines published by Finnra.

Gravel

Tests were carried out on 12 August 2003 to determine the strength properties of the unbound sandy gravel used in the subbase of the test structure. Table 3.3 presents the results of the improved Proctor test for the gravel.

Table 3.3. Results of improved Proctor test on the materials studied.

Material	Maximum dry bulk density /dry density (g/cm3 / kN/m3)	Optimum water content
Sandy gravel	2.168 / 21.26	6.5

The condition variables of the materials (density and water content) were chosen on the basis of the Proctor tests and density measurements of the structure (volumeter, Troxler). The density and water content selected for the tests are presented in Table 3.4.

Table 3.4. Condition variables of the materials used in the modulus tests (target value in brackets).

Material	Dry bulk density (target) (g/cm3)	Water content (target) (%)
Sandy gravel	2.004 (1,994)	5.8 (6.0)

The tests were conducted on one sample using a multi-stage testing procedure. In this method, the sample is loaded until failure on one confining pressure, after which the confining pressure is increased and the sample is again loaded until failure. In this series, the tests were first carried out on four confining pressures: 10, 20, 40 and 80 kPa. At the end of the series, the test was repeated under confining pressure 10 kPa. The confining pressures were affected by creating a partial vacuum (equalling the confining pressure) in the sample.

During the test, in addition to force, vertical and horizontal deformations were measured in the sample so that stresses could be calculated as accurately as possible for the duration of the entire strength test.

The deformation – deviatoric stress curves of the strength tests are presented in Figure 3.3. The confining pressure ($\sigma 3$) – shear strength (τ) points determined from the results are presented in Figure 3.4. Angle of friction and cohesion were determined from the results of the strength tests. Due to the method used, the strength parameters determined represent critical state strength rather than the maximum strength of the material. Examining the test results also shows that the first point does not fit into the pattern – the test was not continued sufficiently long. The points coincide quite well with the straight line, or the development of strength was linear in the stress range used (10 - 80 kPa). The angle of friction and cohesion are determined using the following formulas (3.1–3.2).

$$\tan \phi = S_f / (1 + 2 \cdot S_f)^{0.5} \qquad (3.1)$$

$$c = \tau_0 / (1 + 2 \cdot S_f)^{0.5} \qquad (3.2)$$

in which ϕ is angle of friction (°)
c cohesion (kPa)
S_f inclination of fitted straight line on σ_3 - τ axes
τ_0 intersection of fitted straight line on τ axis

The strength parameters from the test results are presented in Table 3.5. The Table also presents the amended strength properties of base course crushed rock and the materials tested in the HVS Spring Overload study. The analysis uses results from all the tests made on different confining pressures (Figure 3.4). The analysis contains no membrane correction.

Table 3.5. Amended strength parameters of unbound pavements in HVS structures determined by triaxial tests.

Material	Angle of friction (°)	Cohesion (kPa)
Sandy gravel	41.2	8.7
Crushed rock	43.1	43.0
Sand (HVS Spring – Overload)	35.5	12.9
Crushed gravel (HVS Spring – Overload)	44.7	35.6

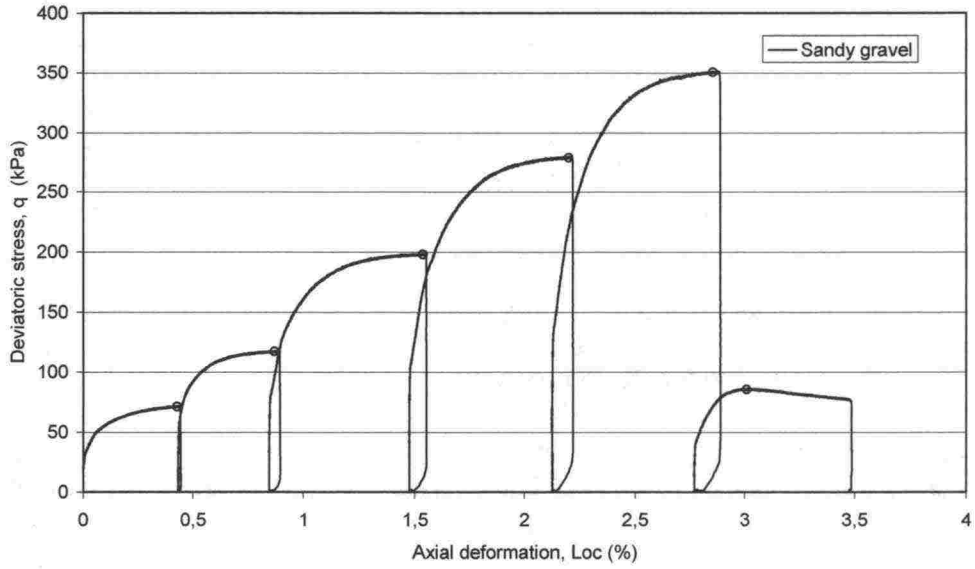

Figure 3.3. Strength test. Development of deviatoric stress in different tests as confining pressure changes.

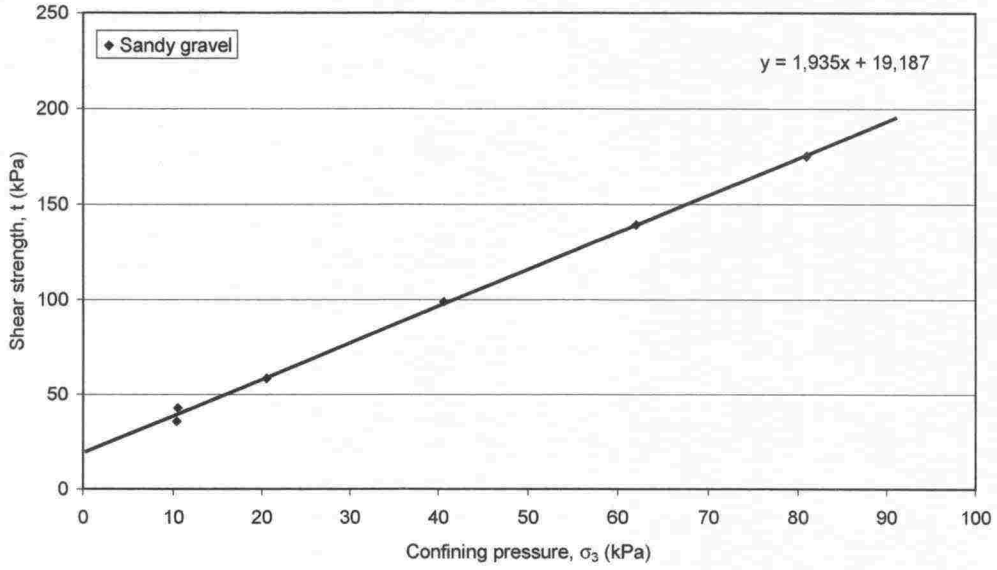

Figure 3.4. Strength test. Determining strength parameters on confining pressure – shear strength axes.

The test conducted on sandy gravel was successful, as Figure 3.4 clearly indicates. The strength parameters produced by the test (such as angle of friction 41.2 degrees) range within the parameters determined previously. Previous tests gave the angle of friction of subgrade sand as 41.9 (amended value 35.5) degrees and that of crushed gravel as 52.3 (amended value 44.7) degrees. The test results show no significant non-linearity. Compared with previous tests, the axial load was restored to zero before applying the confining pressure.

Since the test was conducted practically in the same density and moisture conditions as the previous stiffness and deformation tests of the material in question, the results can be used for analysing HVS tests.

3.2 Laboratory tests for bound materials

The resilient modulus of the asphalt was determined for the test structure's bound wearing course (AB16/100), which consisted of the asphalt layer of the earlier Low-volume roads study test structure and the new layer built on top of it. Stiffness was determined separately for both the lower (Low-volume roads study) and the topmost, new layer.

The tests were conducted according to the Nordic version of the SHRP-P07 protocol. In this method, a cylindrical sample (core drilled from the asphalt layer) is loaded in the direction of the diameter and the dynamic transverse deformations are measured (Figure 3.5). The modulus is determined by a loading procedure based on the indirect tensile test (ITT) with the help of a known loading pulse and dynamic deformations.

The standard shape and timing of the loading pulse is presented in the SHRP-P07 protocol /SHRP-P07 1993/. During loading, the sample is subjected to a combination of a static basic load and a short-term pulse-shaped load. The duration of the sinusoidal pulse is 0.1 seconds and the

interval between pulses 1 or 3 seconds. The static basic load is 10% of the maximum loading pulse. SHRP-P07 proposes a pulse interval of 1.0 second, whereas the Nordic SHRP /FAS 1991, Nordic SHRP 1994/ proposes 3.0 seconds. Unlike the Nordic guidelines, the loading was conducted only at one load level (900 N). The sample was rotated 90° between the loadings. Thus, the result is the average of two results in different directions.

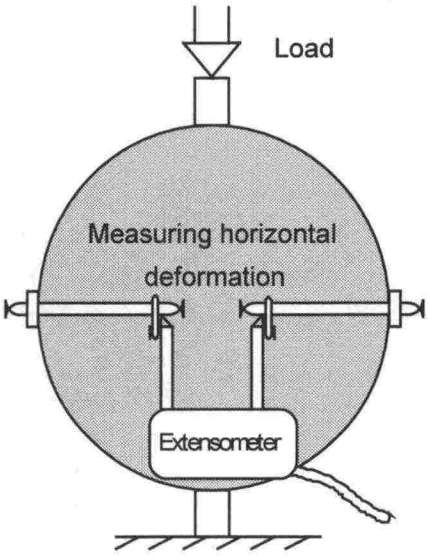

Figure 3.5. Determination of stiffness. Determining the resilient modulus with the ITT test. Illustration of principle.

Three cylinders, 100 mm in diameter, were drilled from the test site from representative spots through the entire bound surface layer, that is, through both asphalt layers. Test cylinders of both the lower and the topmost asphalt layer were sawn from the cylinders. Thus, three parallel samples were obtained from both layers. The thickness of the samples varied between 37.5–60.0 mm. The tests were conducted at a temperature of +10 °C, which was also the temperature used in testing the structures. The value for Poisson's ratio used in the interpretation of the results was $\nu = 0.28$ and the resilient modulus was determined from the difference in the deformation determined from the maximum load and 1 second. The results of resilient modulus determinations are presented in Table 3.6.

Table 3.6. Summary of resilient modulus determinations for the asphalt layers.

Asphalt layer	Topmost, new AB	Lower AB (Low-volume roads study)
Resilient modulus M_r (MPa)	5.360	5.340

The tests showed that the levels of resilient moduli for both layers were the same. The average resilient modulus determined (5.350 Mpa) corresponds to the average levels of moduli previously typically obtained for AB. For instance, the interpolated average for the temperature +10 °C in samples drilled from the SHRP test roads in the early 1990s was roughly 5,700 Mpa.

4 MEASUREMENTS

Deformations, both in the pavements and on the asphalt, tensile strain in the steel grids, earth pressure and changes in moisture content and temperature were monitored during test loading. The responses registered in the measurements were both dynamic and static. The results interpreted on the basis of measurement signals are given in Appendices 3 and 4–7.

Radiometric measurements

Changes in the moisture content of the structures were monitored with radiometric measurements. Each structure contained one radiometric measuring tube, which was used for measurements on different water table levels. There were 9 measurements in all, or 3 from each test structure pair. The measurement results are presented in Appendix 3.

Earth pressure cells

A total of 18 earth pressure cells had been installed in the structures for the Low-volume roads study. Each loading area contained three earth pressure cells at two different depths: in the gravel layer and clay layer. The earth pressure cells had been installed to measure changes in the vertical stress state in relation to the load. The measurements were taken on a bi-directional pass of the test wheel. Maximum values were sought from among the measurement signals and layer-specific earth pressure was calculated as the average of these maximum values. Figure 4.1 gives an example of the measurement signal of an earth pressure cell and determination of the maximum values. Only two of the cells in the gravel layer of structures 26–27 functioned reliably. The measurement results are given in Appendix 5.

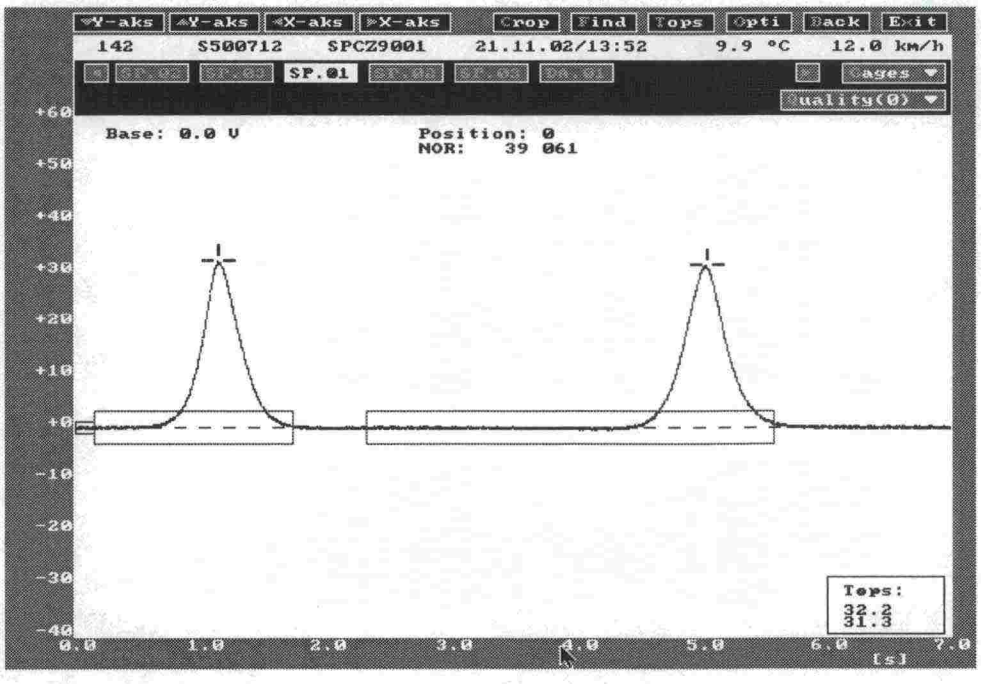

Figure 4.1. Measurement signal of an earth pressure cell and determination of the maximum values.

Emu-Coil sensors

A total of 24 Emu-Coil sensors, or eight in each loading area, had been installed in the structures for the Low-volume roads study. The diameter of the Emu-Coil sensors used was 100 mm. The sensors measured transient and permanent displacements both horizontally and vertically. The measurements were taken on a bi-directional pass of the test wheel. The results give the maximum value from these two measurements as shown in Figure 4.2. There is a large number of measurement results and the maximum value for one pass is determined as the moving average of 20 consecutive measurements. In addition to transient measurements, permanent deformations of the sensors were monitored.

± 1 mm can be considered a threshold value, imposed by measuring technology, for permanent displacements. Displacements smaller than that cannot be reliably determined /Janoo *et al.* 1999/. Displacements in the clay layer varied between 0 and 1.1 mm and exhibited "illogical" behaviour, that is, the displacements diminished as the number of passes increased. This is probably due to the inaccuracy of the measurements for such small displacements. The measurement results are given in Appendix 5.

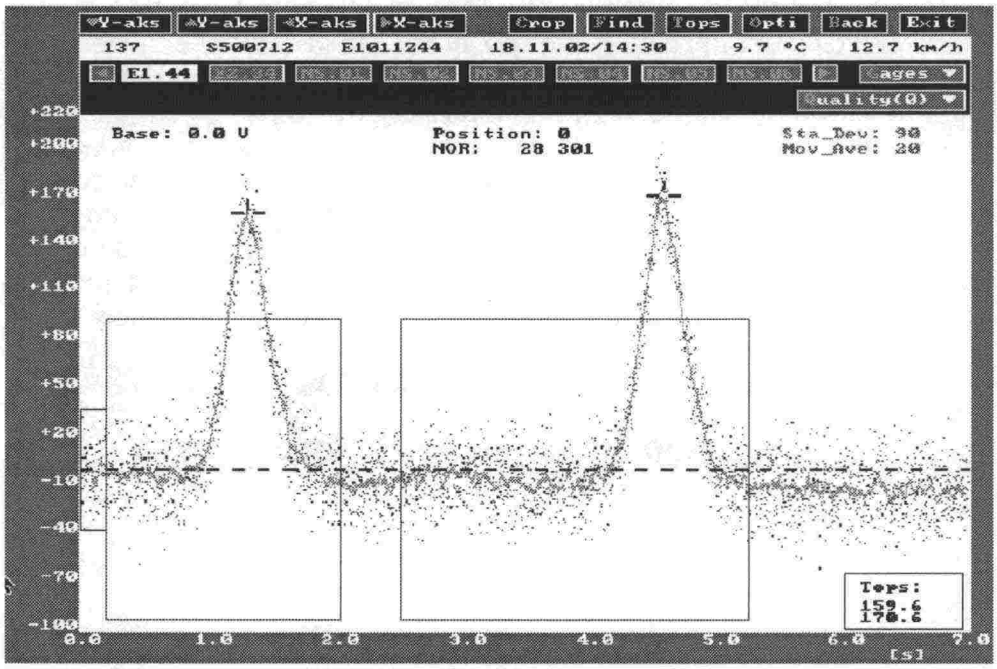

Figure 4.2. Measurement signal of an Emu-Coil sensor and determination of the maximum values.

Accelerometers on the top of the asphalt layer

The deflection of the asphalt layer during the test was monitored with accelerometers installed on the top of the asphalt layer. They were installed in all six structures. The measurements monitored transient strain. The measurement results are given in Appendix 5. Due to reasons associated with the accuracy of the accelerometers and the installation, the measurement results are difficult to interpret.

Horizontal strain gauges in the slope

There were two LVDT displacement gauges, measuring horizontal displacement, installed in the slope of each 8-metre long test structure pair. The gauges were located one in each structure of the pair, in the upper part of the slope, approximately halfway down the crushed rock layer. The gauges were installed resting on purpose-built horizontal supports. The supports were attached to the edge of the concrete basin after the slope was dug open. The gauges were not installed until the HVS had been moved to the test site and the slopes had been dug open. In addition, horizontal displacement of the slope's bend in relation to the edge of the test basin was monitored with reference tacks. The measurement results are given in Appendix 5.

Profilometer measurements of the top of the asphalt layer

Rutting of the pavement's surface was monitored with profilometer measurements from the top of the asphalt layer. Each pair of structures contained three transverse levelling lines to monitor rutting. The profiles were two metres apart so that there was one measuring line in the middle of each structure in a pair and one between the structures. The measurement results are given in Appendix 6.

Strain gauges in the reinforcements

The performance of the reinforcements was monitored with strain gauges. The gauges were only installed to steel reinforcements, as the fastening and functioning of the gauges in fibreglass reinforcement was uncertain. The gauges were installed transversely to the steel grid left of the centre line. There were two gauges on the opposite sides of the steel wire and the tensile strain was calculated as the average of the measurements from these two gauges. There were two instrumented wires in each steel grid test section. The gauges were positioned in three consecutive openings of the tested steel wire as shown in Figure 4.3. Both transient and permanent strain was measured. The measurement results are presented in Appendix 7.

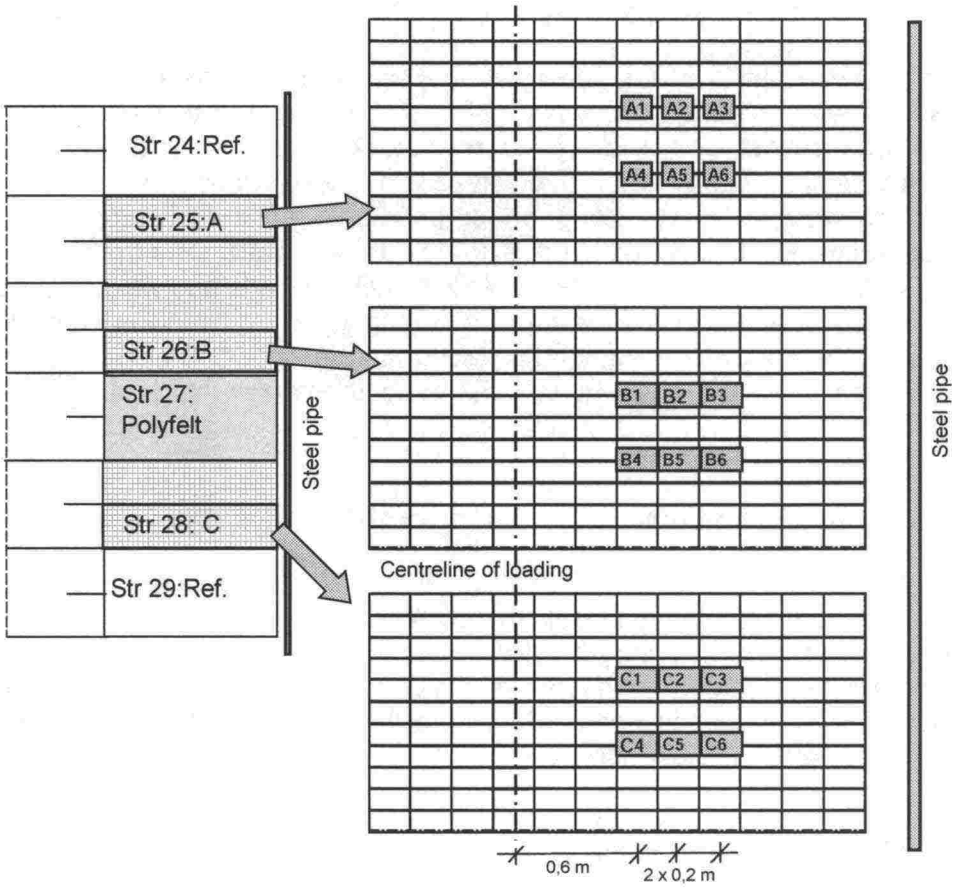

Figure 4.3. Position of the strain gauges.

Distress in the structures

Distress in the structures was monitored during the testing by ocular inspection. No distress other than rutting was observed.

Opening the structures and taking samples after the test

After the test was completed, the structure was lightly protected with frost protective 50 mm EPS plates that were removed in the spring, after the structures had thawed. Before digging the structures open, the research team conducted falling weight deflectometer measurements, the results of which are given in Section 5.9. The structures were dug open and the surfaces levelled. Samples of both unbound and bound pavements were taken on the same occasion. The strength properties of the samples from the unbound layers (clay and gravel) were determined for later calculations. Samples were also sawn from the asphalt layer and the reinforcements for deflection tests and determining the strength properties. While taking samples of the asphalt layer, it was discovered that the asphalt layers of structure 25, in particular, had come apart (Figure 4.4).

Figure 4.4. Asphalt layer sample sawed from structure 25. Asphalt layers have come apart.

The structures were dug open in the middle of the loading area in each pair of structures, that is, at the joining of structure 24 and 25, and so forth. After being dug open, the surfaces of the pavements were levelled. The levelling results, structure by structure, are given in Figures 4.5–4.7. However, only one structure per pair is shown, as there were no great differences within the pairs.

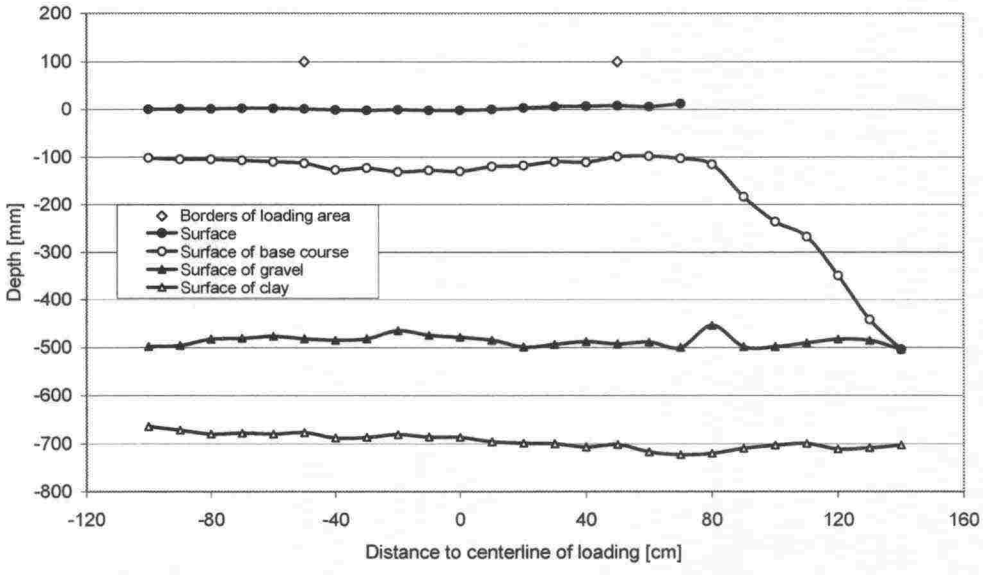

Figure 4.5. Levelling of the tops of the layers after loading in structure 24 (reference structure).

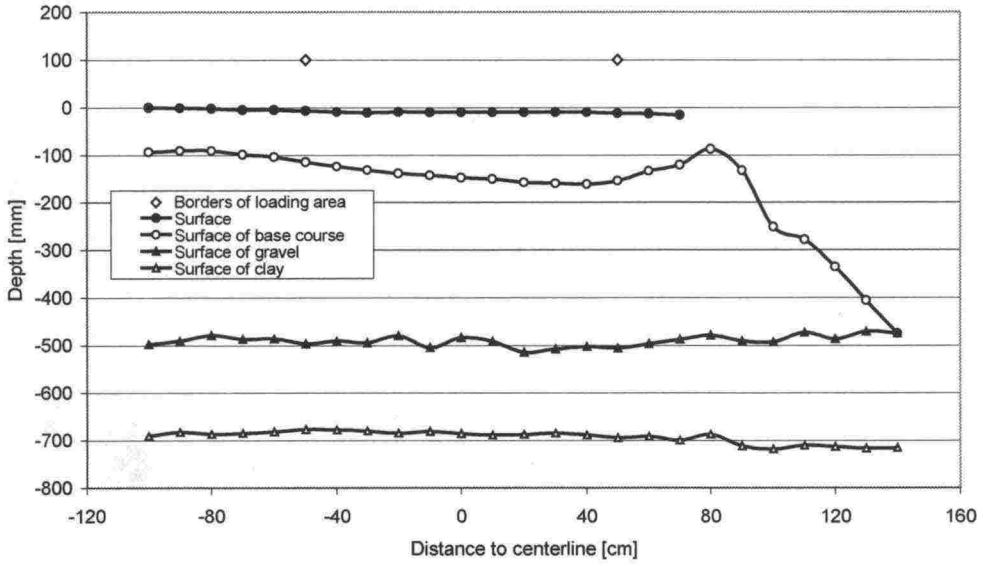

Figure 4.6. Levelling of the tops of the layers after loading in structure 26 (8 mm steel grid).

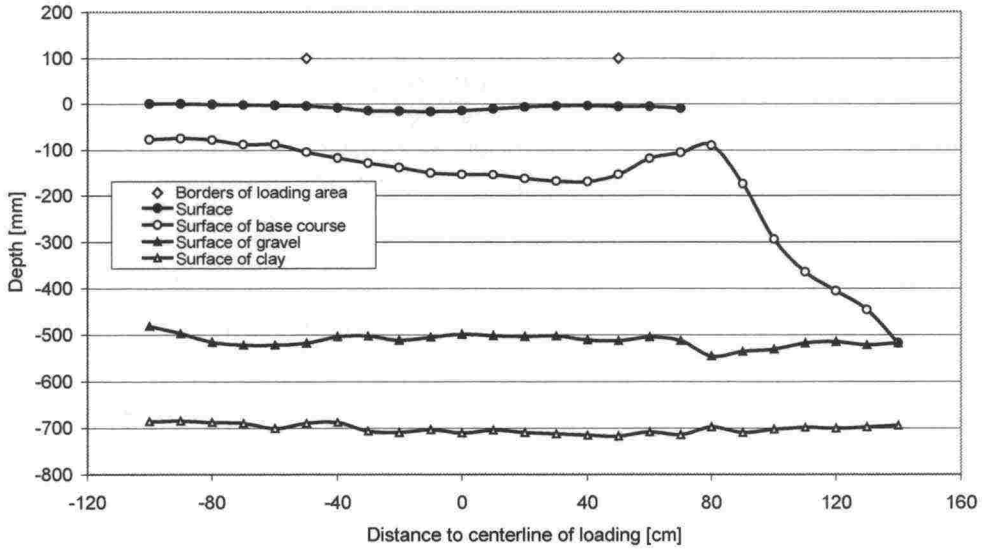

Figure 4.7. Levelling of the tops of the layers after loading in structure 29 (reference structure).

5 ANALYSIS

5.1 The condition of the structures before rehabilitation

In the Low-volume roads study, the structures were designed to correspond to the structure of low-volume roads. Due to the earlier tests, each of the structures was in a different condition. Figure 2.1. shows the new structures and the condition of the structures before rehabilitation. The rut in the steep-sloped structure (28–29) showed a noticeable longitudinal crack, several millimetres wide, towards the centre lane. The other structures showed little distress besides rutting, that is, only a few short, narrow cracks.

The structure was exposed to freezing in winter 2001–2002. After the previous tests were completed, the plug in the bottom of the test basin was opened in order to drain the water from the structures. The winter was relatively mild, but it can nevertheless be assumed that the structures froze during the winter. Comparing the results from the Emu-Coil zero measurements carried out in September 2002 and the final results from the previous tests showed that the sensors had moved 0.03–2.06 mm in relation to each other during the winter and the construction phase. In some places the distance had increased, in some decreased. Although the structures froze, probably no significant loosening occurred during the winter. Thus, it can be said that the structures were more or less in the same condition as they were when the previous test ended.

5.2 Quality of construction

The quality of construction was monitored before and during the rehabilitation with the help of falling weight deflectometer measurements and levelling. The falling weight deflectometer measurements were conducted at water table level W2 (+15.95). They were carried out after both levelling the ruts and spreading the new asphalt layer. The slopes of structures 24–25 and 26–27 were filled up while the slopes of structure 28–29 (steep-sloped structure) were open during the falling weight deflectometer measurements.

Table 5.1 presents the results of falling weight deflectometer measurements at different phases converted to a temperature of +20° C. The Table also includes results of falling weight deflectometer measurements before the previous tests. The deep ruts prevented falling weight deflectometer measurements after the previous tests, therefore the bearing capacity after the tests is an estimate only, based on the results of Loadman tests.

As a rule, the side slopes have been filled during falling weight deflectometer measurements. All bearing capacity measurements in the previous study indicated that the middle structure was the weakest before the test loading, whereas after the tests, structure 28–29 was in the worst condition. After the rehabilitation, the middle structure seemed to give the best bearing capacity measurements. According to the measurements, the bearing capacities of all structures clearly increased after both rehabilitation phases. The measurement results, structure by structure, are presented in Appendix 3.

Figure 5.1 shows the bearing capacities determined from the falling weight deflectometer measurements after levelling the ruts and spreading the new asphalt layer. The Figure also shows the density of the asphalt layer according to DOR measurements. The steel grid can somewhat alter the density values. The lowest average density (2.263 kg/dm^3) and greatest variation (0.042 kg/dm^3) were measured in structure 24–25. The average densities and variations of structures 26–27 and 28–29 were similar (2.352 kg/dm^3 and 0.0375 kg/dm^3).

Table 5.1. Falling weight deflectometer measurements during construction, average bearing capacities E_2 by structures, converted to +20° C.

Measurement date and ground water level	Structure 24–25, MPa	Structure 26–27, MPa	Structure 28–29, MPa
9.7.2001, W1	102	91	93
30.11.2001, estimate	56	34	29
18.9.2002, W2	96	99	94*
24.9.2002, W2	132	134	129*

* = side slopes were open at time of measurement.

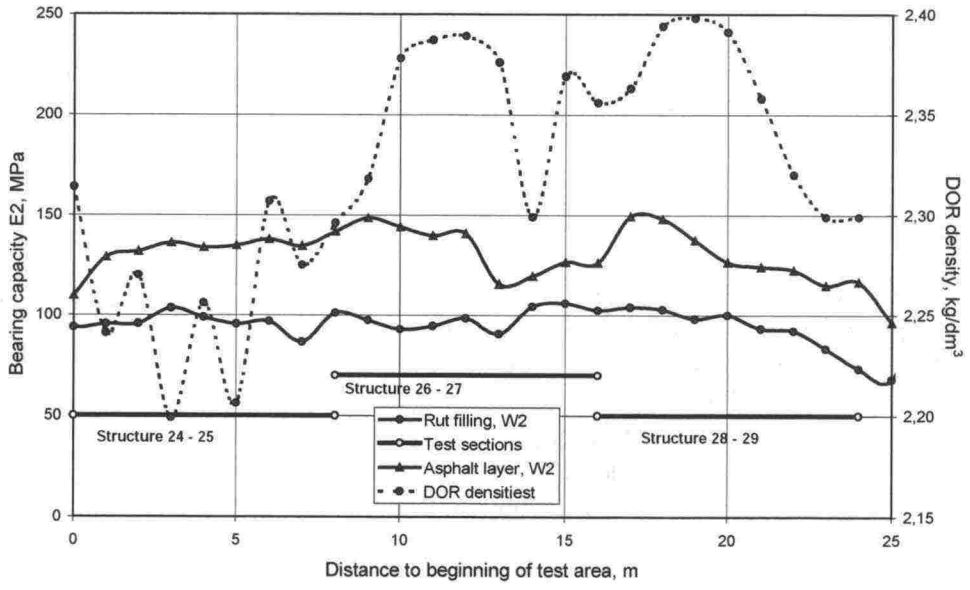

Figure 5.1. Bearing capacity and density measurements during rehabilitation.

Levelling during rehabilitation monitored the thickness of the rut levellings and asphalt layers. Figures 5.2 to 5.4 present the cross-directional thickness of the asphalt layer in different structures. Figure 5.4, furthermore, shows the estimated position of the wide crack resulting from the first phase of loading. The figures are drawn on the assumption that the asphalt layer from the first phase was not deformed or its thickness changed during the first tests. According to the levelling, the total thickness of asphalt layers on the loaded area ± 300 mm from the centreline were:

- structure 24–25: 139 mm
- structure 26–27: 175 mm
- structure 28–29: 188 mm

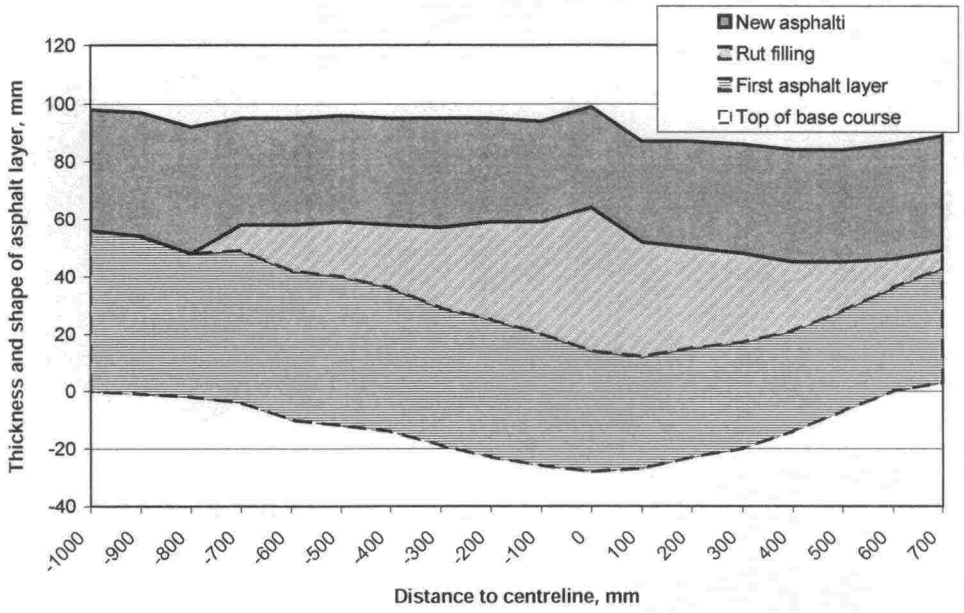

Figure 5.2. Structure 24–25. Cross section of the thickness and shape of asphalt layers at the centreline of the structure.

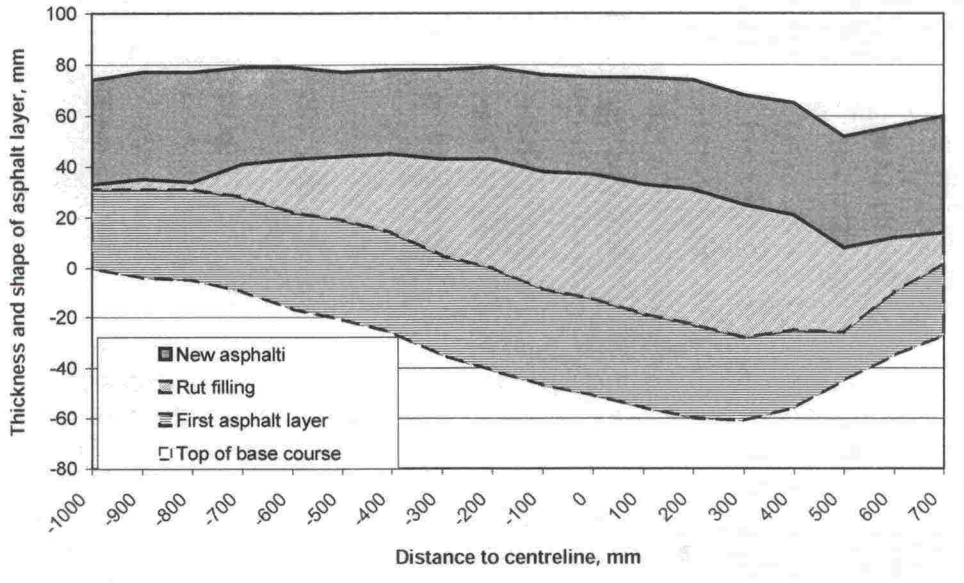

Figure 5.3. Structure 26–27. Cross section of the thickness and shape of asphalt layers at the centreline of the structure.

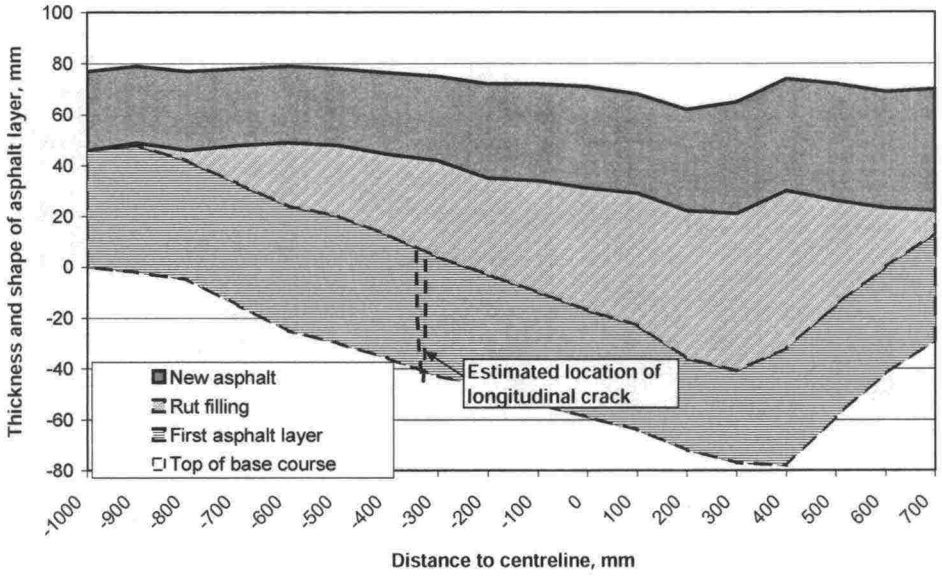

Figure 5.4. Structure 28–29. Cross section of the thickness and shape of asphalt layers at the centreline of the structure.

5.3 The distribution of permanent deformations in the structure

The extent of permanent deformations in the structures was monitored with Emu-Coil sensors. It was assumed that the asphalt layer did not deform as the testing temperature was relatively low (+10° C). The results of, for instance, the tests conducted for the study 'Effect of spring and overload on the rutting of a low-volume road' show that rutting of the asphalt layer was modest /Kivikoski and Laaksonen 2003/. This was the case even though the loading speed used, 12 km/h, is a greater strain from the point of view of deformations than the normal driving speed of 80 km/h.

The Emu-Coil sensors were installed in the structures in the previous testing phase when each test structure was 8 metres long. Furthermore, the sensors were located in pairs in different parts of the structure. Now that the structures were divided into 4-metre strips, the position of the pairs of sensors varied: some were located at the joining of the new structures, some on either side of the joint. The unbound pavements were treated as 8-metre long structures when comparing their deformations. Thus, the rehabilitated pair of structures was treated as one structure and it was impossible to distinguish the effect of the different reinforcements in the results. Due to insufficient measurement results, it was not possible to estimate the extent of deformations in the upper part of the base course.

The displacements in this test were significantly smaller than in the previous test. The results for the Emu-Coil sensors lowest in the clay was not very reliable as regards permanent deformations, because the total deformation was small. The greatest displacements were approximately 1 mm (0.5%). The measurement responses of the horizontal Emu-Coil sensors were also very small and, therefore, the measurement results were unreliable. Figure 5.5 presents the displacements layer by layer at the end of the test. The Figure also shows the results from the first phase tests (Low-volume roads

study) in fainter ink. The test programme as regards changes in the load and the water table level was identical in both phases of the tests, except for the test structure with no slope, in which the water table was not elevated to level W3 in the Low-volume roads study. However, the number of load repetitions in the second phase tests was double that of the first phase. Despite this, the displacements were smaller than in the first phase tests (Low-volume roads study).

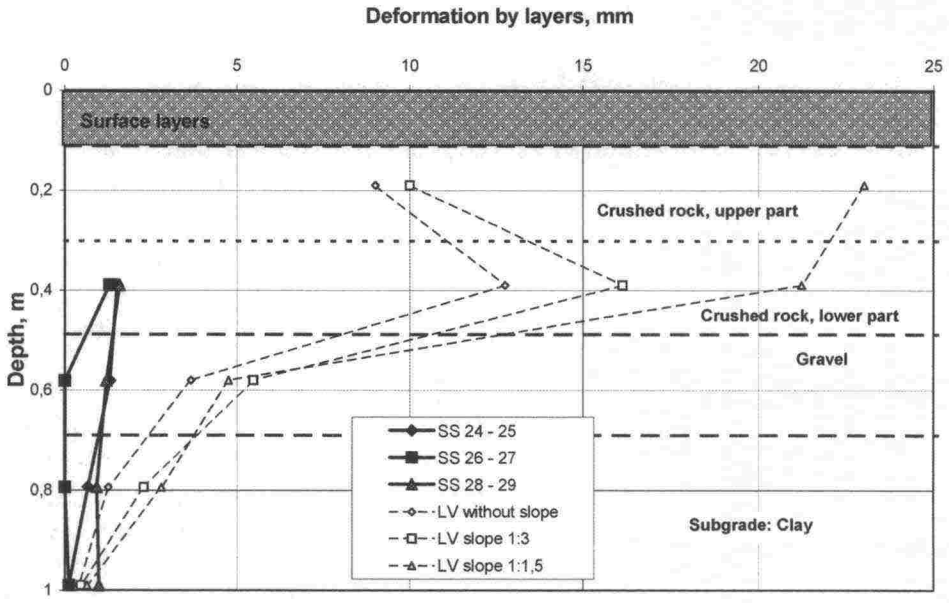

Figure 5.5. Vertical displacements in different tests.

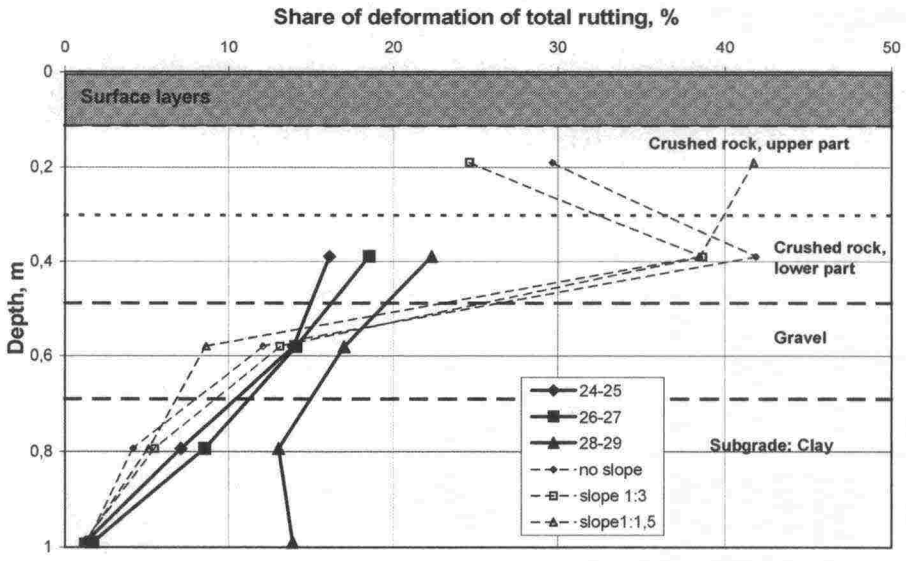

Figure 5.6. Share of vertical displacement of pavement in the total rutting of the surface.

Figure 5.6 presents the share of different layers in the total rutting. The data for the upper part of the base course could not be determined sufficiently

reliably due to inadequate measurement results. However, subsequent measurements of the structures clearly indicated that the majority of deformations had occurred in the base course (Figures 4.5–4.7). According to the Emu-Coil measurements, the lower part of the base course accounted for 16–22%, the gravel 13–17%, upper part of the clay 7–13% and slightly lower parts of the clay for 1–14% of the total rutting. It is probable that by far the largest deformations in this test occurred in the upper part of the base course. Some of the remaining deformations occurred lower in the clay. The distribution of deformations differs from that of the first phase, in which the upper and lower parts of the base course deformed more or less equally (Figure 5.6).

The difference in the distribution is probably due to the fact that thicker asphalt layers distribute the load more efficiently and over a larger area. The properties of the pavements of a low-volume road with a thin asphalt layer have a greater effect on total rutting than those of a road with a thicker asphalt layer. On the other hand, the limits for permissible deformations on roads with thicker asphalt layers are tighter and impose greater demands on the deformation properties of unbound layers.

The clearly smaller deformations in the rehabilitated structures are also significant. Although the gravel layer's earth pressure in the rehabilitated structures also decreases 42–58% (Figure 5.11), the deformations decrease even more in proportion, 65–82%. The decrease in the earth pressure in the clay layer is slightly less, 38–48% (Figure 5.12), and the corresponding decrease in deformations 47–74%. It is easy to see from this ratio that the relation between deformations and stress state is non-linear.

Changes in the load or moisture content did not have a significant effect on the vertical deformation distribution. Figure 5.7 shows the vertical displacements in structure 24–25 under different loads and at different water table levels. The distribution showed an identical shape on all structures.

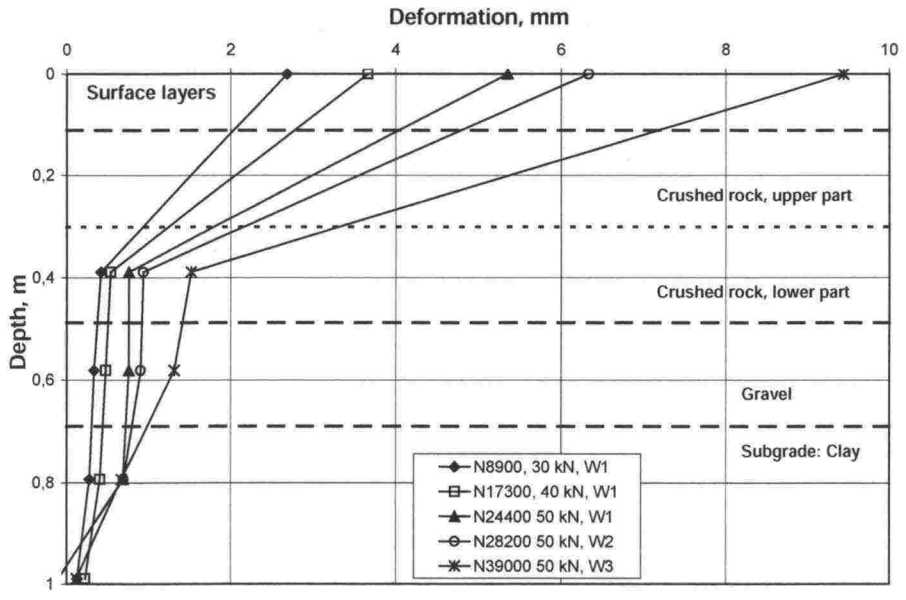

Figure 5.7. Structure 24–25. Changes in vertical displacements under different loads and at different water table levels.

The level of deformations in unbound layers remained low, as Figure 5.8 indicates. It is not possible to determine the threshold value for plastic performance (shakedown value) for different loads or moisture contents on the basis of the results for this test alone. Figure 5.8 also shows the deformations of the corresponding structures in the first test phase. The threshold value can be roughly estimated from the combined results of these two tests. No great differences were observed in the ratio of deformations between the different structures. The Figure does not show the ratio of deformations in the preloading stage. Instead, it only presents the stage of 'decelerating' performance.

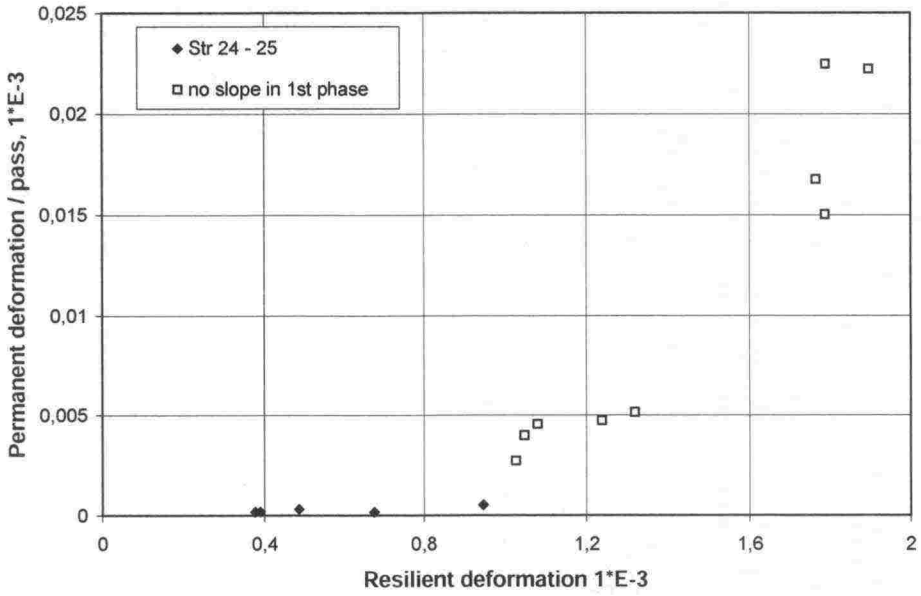

Figure 5.8. *Structure 24–25. Ratios of permanent and transient vertical displacement in the crushed rock layer in this and the Low-volume roads study.*

5.4 Rutting of the structures

The rutting of the structures' surfaces was monitored with profilometer measurements. Each 8-metre long loading area had three transverse profilometer lines. The measuring lines were positioned so that there was one line in the middle of each structure and one between the structures. Figure 5.9 shows a longitudinal section of the structure's surface on the centreline of loading before and after the test and the positions of the profilometer lines. Thus, the deepest rut was not necessarily situated at the measuring line.

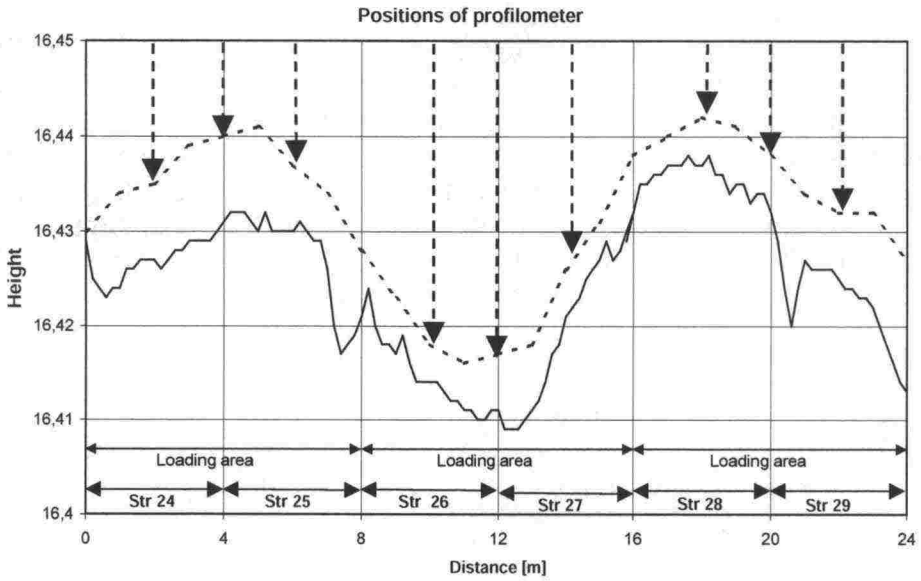

Figure 5.9. Longitudinal section on the centreline of loading before and after the test and the positions of the profilometer lines.

The rutting of the structures' surfaces was monitored with the profilometer line situated in the middle of each structure (Figure 5.10). Structures 24 and 29 were unreinforced reference structures. Structures 25 and 28 contained steel grid 1 (6 mm transverse wire), structure 26 steel grid 2 (8 mm transverse wire) and structure 27 fibreglass reinforcement.

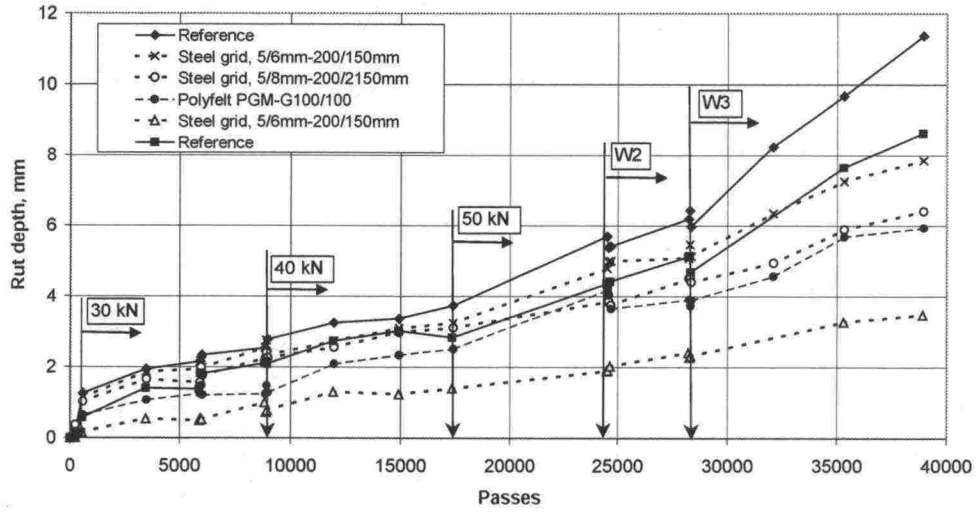

Figure 5.10. Rutting of the surfaces of the structures.

The unreinforced reference structures showed the deepest ruts at the end of the test. Clearly the slowest structure to become rutted was structure 28, which contained the steel grid with 6 mm transverse wire. On the other hand, structure 25, with an identical steel grid, rutted nearly as fast as the unreinforced reference structure 24. The structures on the centremost loading area, with an 8 mm steel grid and fibreglass reinforcement, rutted almost equally fast.

Comparison between structures 25, 26 and 27 shows that the differences between the grids studied were small. It can, therefore, be concluded that the grids studied performed equally well.

The structure pair 28–29 corresponds best to a situation in which a road structure with a steep slope is rehabilitated, as the structure pair previously had a steep slope. In the other structures, the slope was made steeper or built only just before test loading. The reinforced structure in the pair 28–29 was clearly the slowest to become rutted, although on the outset, the loading area was in the poorest condition and it had a deep longitudinal crack. On the other hand, due to thicker patching over the previous ruts, the total thickness of the asphalt layers was clearly the highest, 188 mm – 139 mm. In this pair, the difference in rut depth between the reinforced and unreinforced structures at the end of the test was also the greatest, approximately 3:1. On the other hand, in the structure pair 24–25, the difference in rut depth between the reinforced and unreinforced structure was significantly smaller, approximately 34%. This great difference between the structure pairs 28–29 and 24–25 is probably partly because the condition of structure 24–25 was better before the rehabilitation. Another explanation could be that the previously slopeless structure of the pair 24–25 was changed into one with a steep slope and some of the deformations were due to this.

At this stage, the results seem to indicate that the thickness of the wire in the steel grid has no effect on rutting speed. In other words, the capacity of the steel grid with thinner wire is great enough to receive the mobilised stress without major deformations. Furthermore, it seems that the worse the condition of the original structure the better the reinforced structure performs.

5.5 Earth pressures

Earth pressures in the structures were only monitored in the gravel and clay layers. The measurements monitored three parallel earth pressure cells and the results are averages of these measurements. The pressure cells were installed during the Low-volume roads study and their position varied underneath the different structures. In structure pairs 24–25 and 28–29, the pressure cells were only located under structures 25 and 28. There were two pressure cells under structure 26 and one under structure 27. This is why earth pressure is treated as an average function of each of the 8-metre long structures and the effect of the reinforcements has not been specified.

Figure 5.11 shows the ratio of gravel layer earth pressures in the first phase (Low-volume roads study) to the rehabilitated structure on different load levels while Figure 5.12 shows the same for the clay layer. The earth pressure was measured while the structure was loaded.

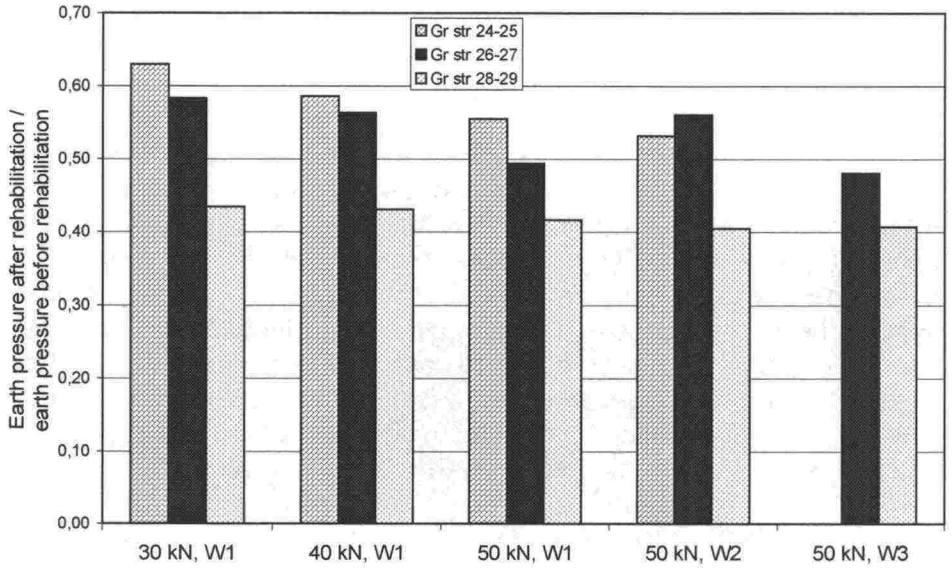

Figure 5.11. Ratio of earth pressure while loaded, top of the gravel layer (depth approximately 500–600 mm) (after/before loading).

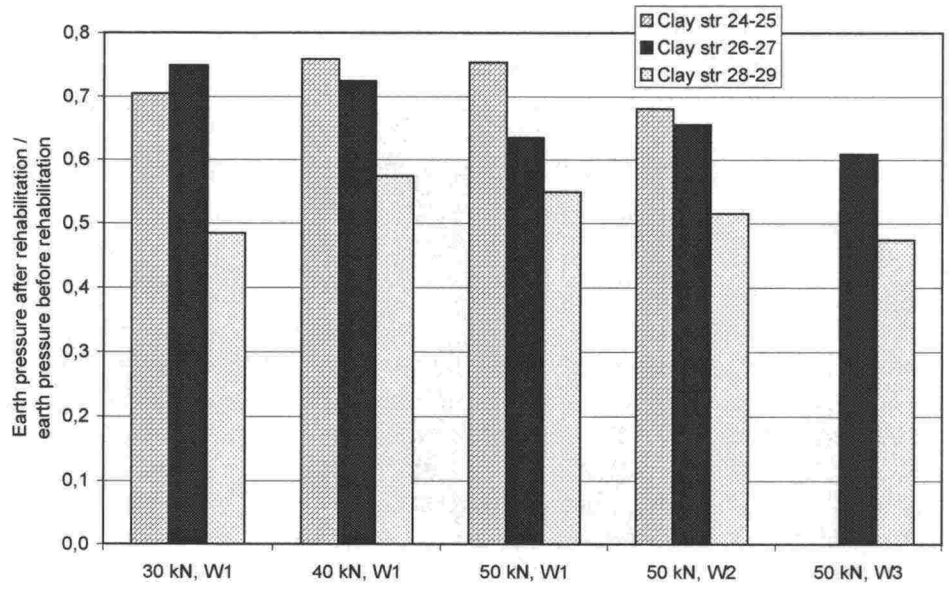

Figure 5.12. Ratio of earth pressure while loaded, top of the clay layer (depth approximately 700–800 mm) (after/before loading).

Earth pressure in the gravel layer in the rehabilitated structure decreases on average 42–58% (Figure 5.11). The average decrease in the earth pressure in the clay layer is slightly less, approximately 28–48% (Figure 5.12). The Figures show that the relative decrease in earth pressure was the greatest in structure 28–29 (58% in gravel and 48% in clay). This is probably because the shape of the structure (slope steepness) did not change and, therefore, the structure best shows the effect of the rehabilitation. The earth pressure of the other structures is influenced not only by the increase in the thickness of the asphalt layer, but also the change in the cross-section of the structure, from no slope or gentle slope to steep slope.

5.6 Tensile strain in steel grids

Both permanent and transient tensile strain was monitored in the steel grids. According to the measurements, the load corresponding to permanent tensile strain in the steel grids varied between 6.7–13.9 kN/m in structures 24–25, between 5.0–13.6 kN/m in structures 26–27 and between 0.1–3.4 kN/m in structures 28–29. Thus, a relatively small permanent load had mobilised in the steel grid, and the tensile strains remained relatively small, max. 600 µstrain. The mobilised stresses were so small that the diameter of the steel grid wire was insignificant.

The load on the grids was calculated using the following equation (5.1).

$$F = E_s \cdot \varepsilon_s \cdot A_r \qquad (5.1)$$

in which F is force in steel wire, kN
E_s elastic modulus of steel, 200 GP = 200 000 kPa
ε_s tensile strain of steel
A_r cross section of steel wire, m^2.

Load has very little effect on the tensile strain observed in the steel grid. According to measurements, the additional tensile strain in the steel grid caused by load is typically only 10% of its permanent tensile strain.

5.7 Permanent horizontal displacements

The horizontal displacement of the slope was measured from the top of the structure and the middle of the base course. Horizontal displacements exhibit the same phenomenon as vertical displacements: the vertical displacements were clearly smaller than the corresponding displacements observed in the Low-volume roads study. The greatest horizontal displacements of the structure with 1:1.5 slope in the Low-volume roads study were in the order of 21 mm. Figure 5.13 shows the horizontal displacements in structure 24 on different load levels. On the basis of the measurements, it would seem that in this test, the horizontal displacements do not concentrate in the top part of the base course as clearly as was the case in the Low-volume roads study. However, there were only two measurement levels in this test and the deformations were small, so the conclusions are only tentative.

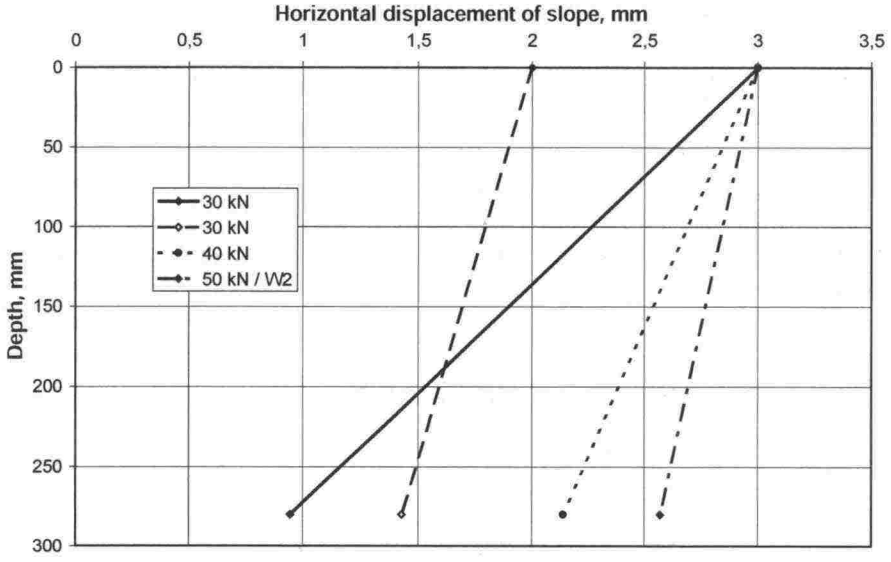

Figure 5.13. Permanent horizontal displacements in structure 24 on different loads.

5.8 Falling weight deflectometer measurements

Falling weight deflectometer measurements were carried out before and after testing. The results are presented in Table 5.2. The bearing capacity values for the fibreglass reinforcement are clearly the smallest, while the index values were the highest. The differences between the bearing capacities of reinforced and unreinforced structures were small (1–22%). The differences in the values of the SCI indices, describing the shape of the deflection basin, were slightly higher (0–25%), when comparing only the steel grids. Comparing the structure pairs 24–25 and 28–29, the greater differences in bearing capacity and SCI indices in structure pair 28–29 indicate better performance of the reinforcement.

Other studies have also come to the conclusion that falling weight deflectometer measurements do not reveal great differences between reinforced and unreinforced structures. Therefore, the better performance of a reinforced structure cannot be reliably measured with a falling weight deflectometer. It is possible that the SCI index could give a slightly more reliable value, but it would also be only an estimate.

Table 5.2. Surface bearing capacity values and SCI indices calculated from falling weight deflectometer measurements (before/after testing).

Test	FWD surface bearing capacity	SCI300 (µm)	SCI450 (µm)
Str 24 (reference)	128 / 98	411 / 564	542 / 772
Str 25 (steel grid 6 mm)	136 / 105	397 / 566	504 / 747
Str 26 (steel grid 8 mm)	142 / 102	371 / 585	472 / 775
Str 27 (Polyfelt PGM-G100/100)	125 / 114	467 / 511	592 / 667
Str 28 (steel grid 6 mm)	138 / 104	394 / 578	499 / 764
Str 29 (reference)	120 / 85	446 / 716	572 / 960

5.9 Condition of the structures after the test

Samples for deflection tests and determining the resilience properties were sawn off when the structures were dug open. At this point, it was discovered that the steel grid had sunk into the new asphalt layer. In the steel grid structures, the new and old asphalt layers had adhered to each other only poorly. Particularly in structure 25, the new asphalt layer was completely unattached to the old asphalt layer (Figure 4.4). The asphalt layers adhered to each other well in the structure with fibreglass, in which the reinforcement was glued with bitumen emulsion. As for the unreinforced structures, the asphalt layers in structure 24 adhered clearly more poorly than in structure 29. This factor can partly explain the great difference in the rutting behaviour of the structure pairs 24–25 and 28–29. It is also possible that sawing may have contributed to the separation of the asphalt layers from each other.

5.10 Estimating the lifetime of the structures

The test structures rutted noticeably slower than it was estimated on the basis of the original structures. The study aimed at achieving a rut of 15 mm in the structure with the deepest ruts. The loading programme was the same as in the first phase, although the number of load passes was doubled at each loading stage. This means that the number of load passes, which in the first phase was 18,000, was raised to approximately 39,000 in the second phase. Although the number of load passes was raised, profilometer measurements showed that the deepest rut was only approximately 12 mm. However, due to the schedule of the heavy vehicle simulator, the test could not be continued until achieving the target depth of 15 mm used as the starting point for design. Approximately four more weeks would have been necessary (20,000 passes per shift).

The service life of structures – here the number of passes – can be estimated with the help of different extrapolations. The aim was to discover the structure's service life corresponding to a rut depth of 15 mm. The extrapolations were conducted on the basis of the last loading stage, in which the wheel load was 50 kN and the water table level W3, that is, the ground water reached the middle of the base course. The greatest uncertainties in the estimation are related to structures with shallow (under 5 mm) ruts.

A. Linear extrapolation

The simplest way to carry out the extrapolation is to continue rutting at the same speed (linear extrapolation). In this estimate, the rutting speed is determined on the basis of the difference of the last two observations (Equations 5.2 and 5.3). The calculation results are given in Table 5.3.

$$N_{15\,mm} = N_{lopp} + \frac{(15 - u_{lopp})}{v_{lopp}} \qquad (5.2)$$

$$v_{lopp} = \frac{(u_n - u_{n-1})}{(N_n - N_{n-1})} \qquad (5.3)$$

in which N_{15mm} is number of passes corresponding to a rut depth of 15 mm
N_{lopp} number of passes at the end of the test
N_n number of passes at observation n (here the end of the test)
N_{n-1} number of passes at observation immediately before n
u_{lopp} rut depth at end of test
v_{lopp} rutting speed at the last observation interval, mm per pass
u_n rut depth at observation n, mm
u_{n-1} rut depth at observation immediately before n, mm

B. Extrapolation based on a power function

Linear extrapolation does not take into account the deceleration of rutting as the number of passes increases. That is why a non-linear extrapolation based on a power function was also carried out. The extrapolations were carried out with Excel spreadsheet software by fitting the power function to all the observations (3 to 4 observations) of the last loading stage (load 50 kN, water table level W3) by searching for the smallest value of the sum of squares of the difference of the results. The power function used was of the form in 5.4. The results of the calculations are given in Table 5.3.

$$u = A \cdot N^B + C \qquad (5.4)$$

in which u is rut depth, mm
A,B,C regression parameters
N number of passes

The parameter B is also called the age index. The small number of measurement results posed a problem for fitting the curve to the results of this test, leading to increased uncertainty and decreased reliability of the extrapolation. The shape of the power function curve depends heavily on the value of parameter B. If the parameter B is given the value 1, the solution is reduced to the linear solution. If the index is given a value above 1, rutting accelerates, whereas if the value given to the index is less than 1, rutting decelerates. It can be assumed that in these tests the rutting decelerates, as the total deformations remain at a low level.

Table 5.3. Number of passes resulting in a rut depth of 15 mm for different extrapolation functions.

Test	A. Linear fitting	B. Power function fitting
Str 24 (reference)	45,350	46,300 ($u = 0.00161*N^{0.895}-9.17$)
Str 25 (steel grid 6 mm)	64,400	66,800 ($u = 0.00081*N^{0.900}-2.81$)
Str 26 (steel grid 8 mm)	89,100	87,300 ($u = 0.00147*N^{0.825}-2.51$)
Str 27 (Polyfelt PGM-G100/100)	102,000	87,700 ($u = 0.0831*N^{0.505}-10.94$)
Str 28 (steel grid 6 mm)	146,200	194,500 ($u = 0.0280*N^{0.538}-4.80$)
Str 29 (reference)	61,750	66,800 ($u = 0.2406*N^{0.437}-15.67$)

According to these results, the value of the age index varied between 0.44–0.9. The range of variation is great and heavily dependent on the number of measurement results. It can be assumed that if there were more measurement results over a longer period of time, the value of the age index would decrease. The results seem to indicate that the condition of the structure before the rehabilitation affects the value of the age index. According to Finnra's data on the condition of roads, the age index B of the power function usually varies between 0.2–0.25 when the traffic volume is a maximum of 800 vehicles per 24 hours.

There were too few measurement results from the last loading stage for the interpretation to be reliable. There was an experiment to fit the curve so that the results for the previous water table level would also be included, but the reliability of the results suffered considerably. The age indices varied within the same range as before or they increased.

When comparing unreinforced reference structures and reinforced structures, it can be concluded that the rutting speed of a reinforced structure is slower than that of an unreinforced structure. According to this comparison, the rutting of reinforced structures reduces by 40–150%, which corresponds to an increase of 40–190% in the structure's service life. The reinforcements were especially effective in the structure pair 28–29, which was in the poorest condition at the outset, but the shape of which was not changed during the tests. The different performance of corresponding structures is probably also due to how well the asphalt layers adhere to each other (see Section 5.9). No major differences were perceived in the rutting speeds of the different reinforcements.

6 CONCLUSIONS AND SUGGESTIONS FOR FURTHER RESEARCH

The rehabilitation of structures tested and rutted in the Low-volume roads study was successful. The structures had rutted and damaged in different ways during the previous tests. Rehabilitation of the structures evened out the differences in the condition of the structures, because after rehabilitation, the bearing capacities measured with a falling weight deflectometer showed no major differences between the structures. The bearing capacities increased significantly in all structures. In fact, they more than doubled compared to the original situation.

Laboratory tests show that the properties of the asphalt layer to be rehabilitated were the same as those of the asphalt layer constructed a couple of years earlier. The strength tests conducted on the unbound pavements and subgrade seem reliable and characteristic of the materials in question. The strength and deformation properties will be utilised more extensively in modelling conducted at a later date.

The unreinforced reference structures showed the deepest ruts at the end of the test. Clearly the slowest structure to become rutted was structure 28, which contained the steel grid with 6 mm transverse wire. On the other hand, structure 25, with an identical steel grid, rutted nearly as fast as the unreinforced reference structure 24. The structures on the centremost loading area, with an 8 mm steel grid or fibreglass reinforcement, rutted almost equally fast.

It would seem that the thickness of the wire in the steel grid had no effect on rutting speed in this case. In other words, the capacity of the steel grid with thinner wire is great enough to receive the mobilised stress without major deformations. Furthermore, it seems that the worse the condition of the original structure the better the reinforced structure performs.

The earth pressure values for unbound layers showed a clear decrease due to the rehabilitation of the structures. The earth pressure of the gravel layer in the rehabilitated structure decreased 42–58%. The decrease in the earth pressure in the clay layer was slightly less, approximately 38–48%. The structures the cross section of which was changed in connection with the rehabilitation showed a smaller decrease in earth pressure than the structures that retained their shape.

The distribution of permanent deformations mainly conformed to that of the Low-volume roads study. However, the share of permanent deformations decreased significantly after rehabilitation, despite the slope being made steeper.

The different rutting behaviour of the various pairs of structures can be explained by the different condition of the structures before rehabilitation, the varying thickness of the asphalt layers and the varying degrees of adhesion between the asphalt layers. The effect of the adhesion between the asphalt layer and the reinforcement on the service life and design of the structures will be the subject of a further study.

These findings can be summarised by saying that using various reinforcements in the rehabilitation of low-volume roads can clearly extend the service life compared to unreinforced rehabilitation. The extension of service life achieved is case- and site-specific, depending on the condition of the old surface structure, properties of the rut levelling, the reinforcement used and the new asphalt, but most of all how all of these factors function together. The test results allow us to indirectly estimate that the adhesion of the reinforcement to its base and the new surface layer on the one hand and the mutual adhesion of the old and new surface layers on the other can have a very significant effect on the extension of service life achieved. Adhesion could be the single most important factor explaining the great relative improvement observed elsewhere – even greater than in this study – in the service life of a road when using reinforcements. Therefore, it is highly advisable to study the effect of adhesion in more detail.

7 APPENDICES

Appendix 1 Map and cross sections of test site
Appendix 2 Quality control measurements during construction
Appendix 3 Radiometric measurements
Appendix 4 Earth pressure measurements
Appendix 5 Deformation measurements
Appendix 6 Profilometer measurem,,ents
Appendix 7 Strain measurements of reinforcements

APPENDIX 1 MAP AND CROSS SECTIONS OF TEST SITE

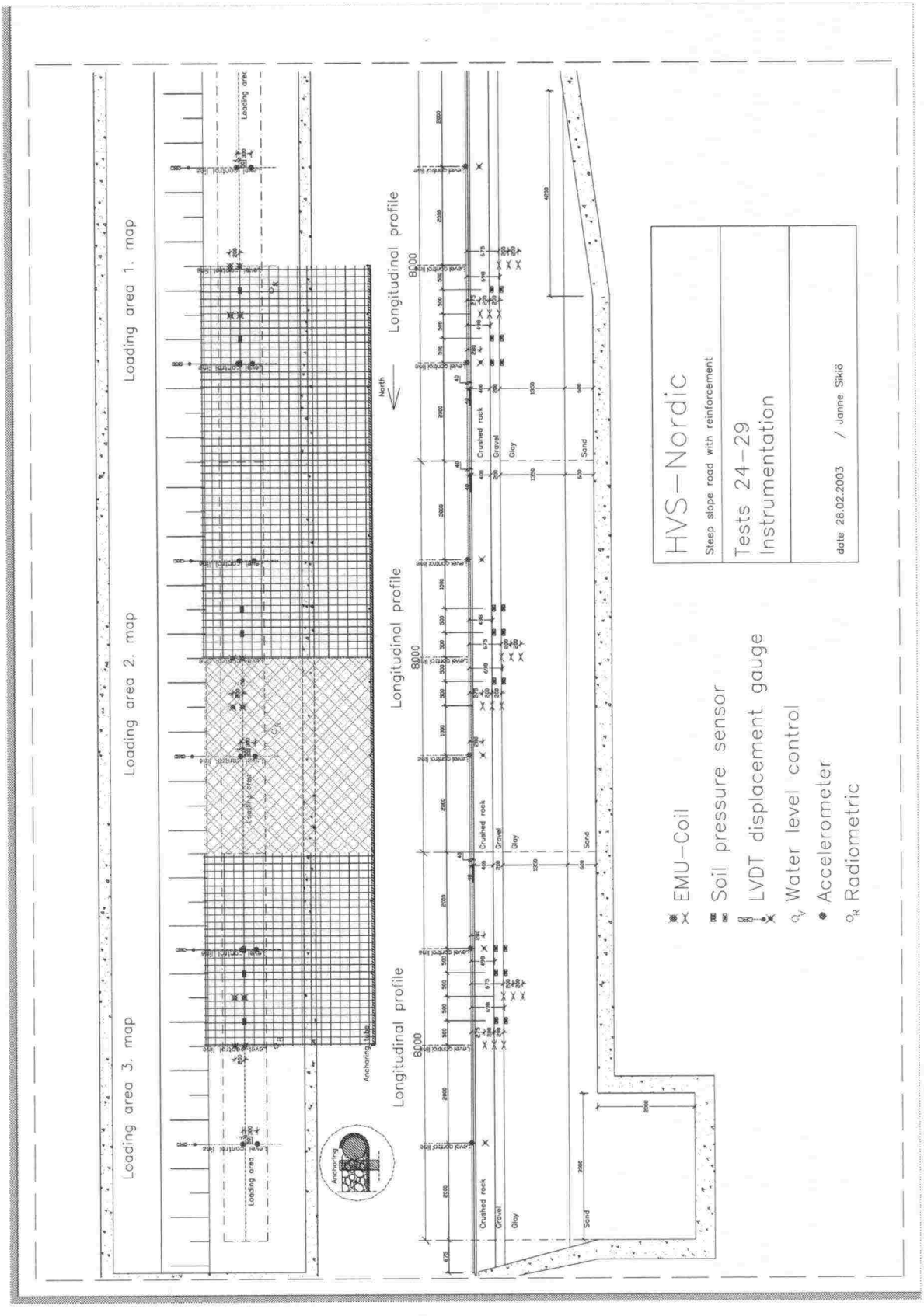

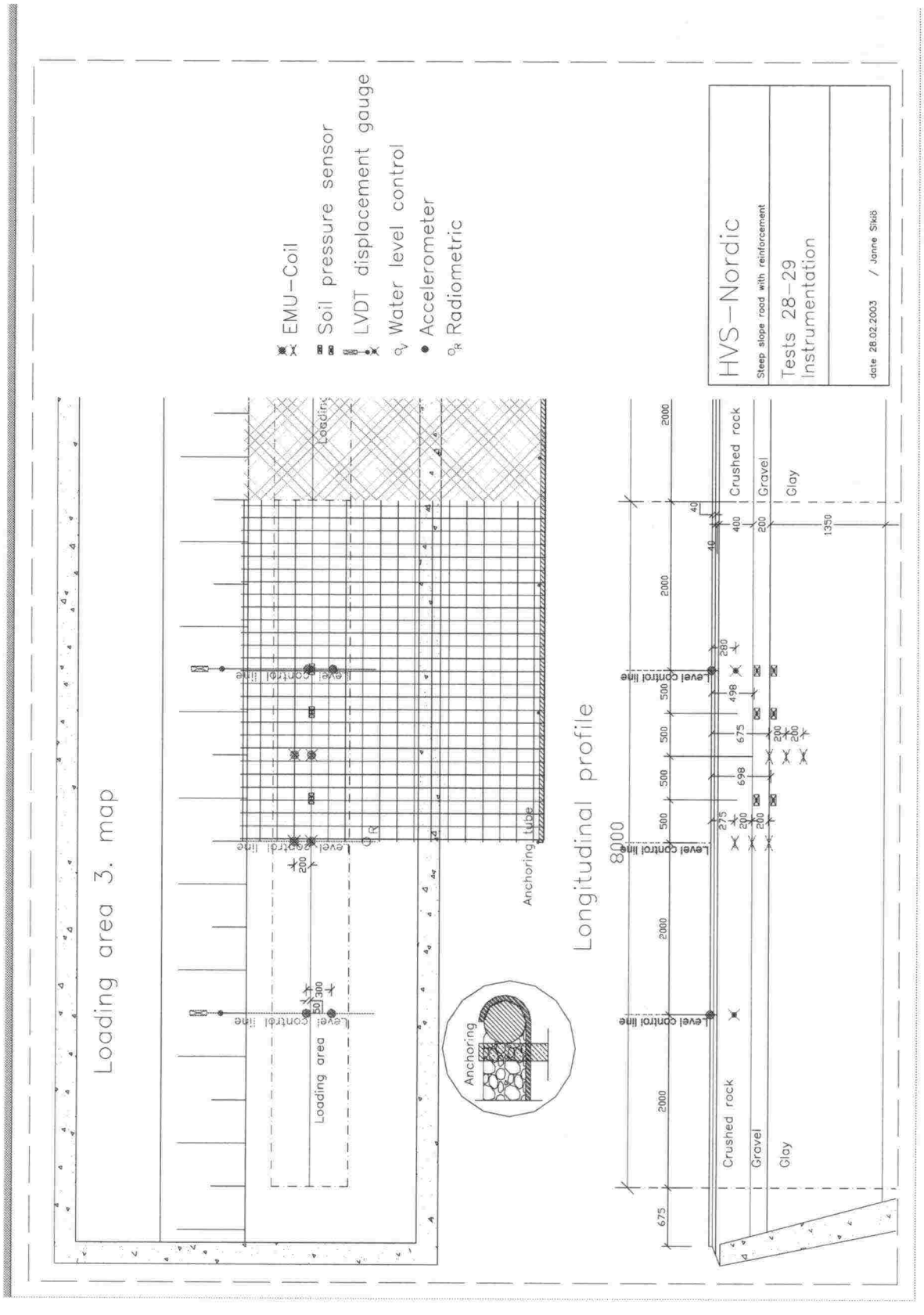
EMU-Coil
Soil pressure sensor
LVDT displacement gauge
Water level control
Accelerometer
Radiometric
HVS-Nordic
Steep slope road with reinforcement
Tests 28-29
Instrumentation
date 28.02.2003 / Janne Sikiö
Loading area 3. map
Loading area
Level control line
Anchoring tube
Anchoring
Longitudinal profile
8000
Crushed rock
Gravel
Clay
2000
675
1350
40
400
200
260
498
500
675
698
275
300
150

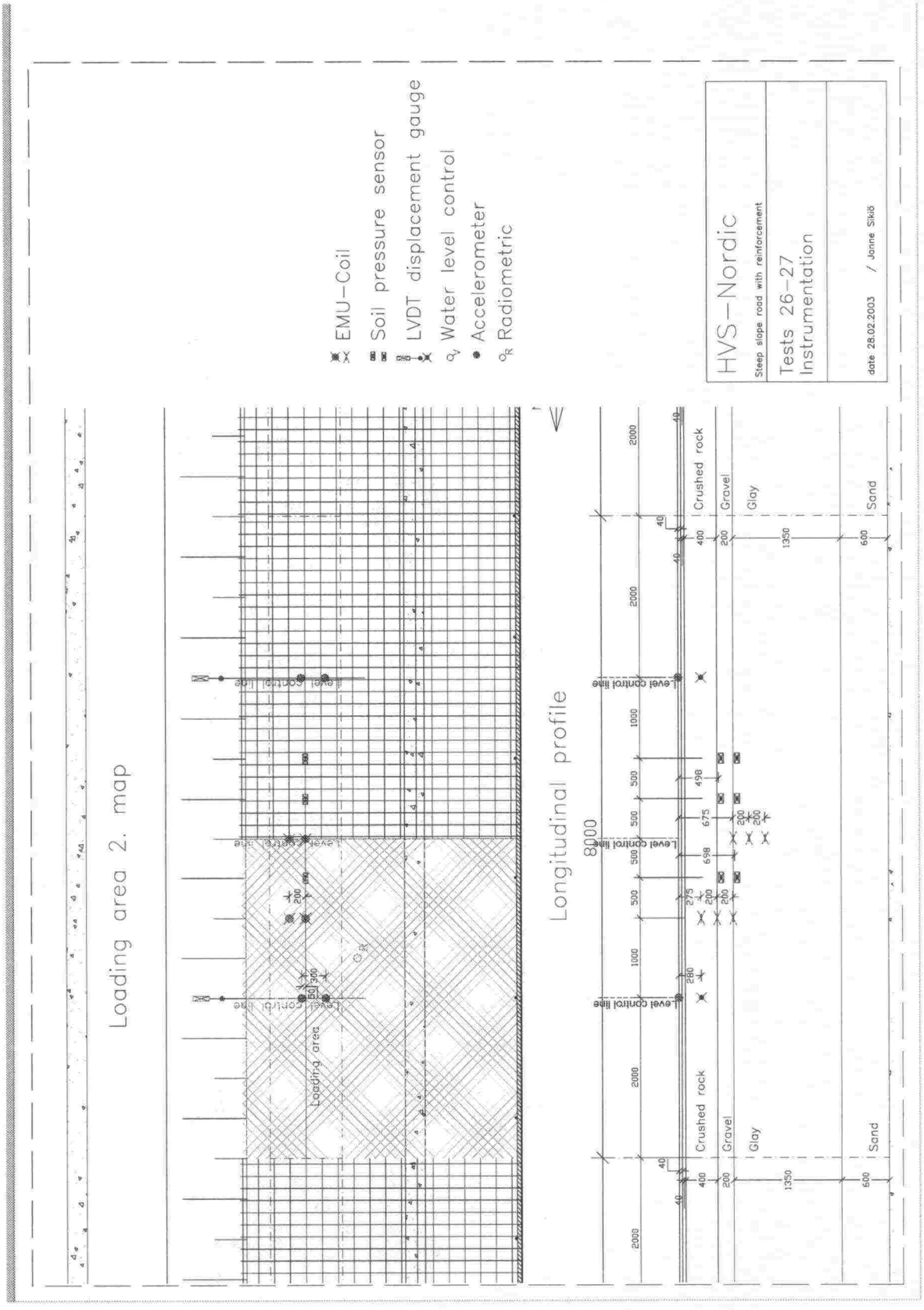
EMU–Coil
Soil pressure sensor
LVDT displacement gauge
Water level control
Accelerometer
Radiometric
HVS–Nordic
Steep slope road with reinforcement
Tests 26–27
Instrumentation
date 28.02.2003 / Janne Sikiö
Loading area 2. map
Loading area
Level control line
Longitudinal profile
8000
Crushed rock
Gravel
Clay
Sand

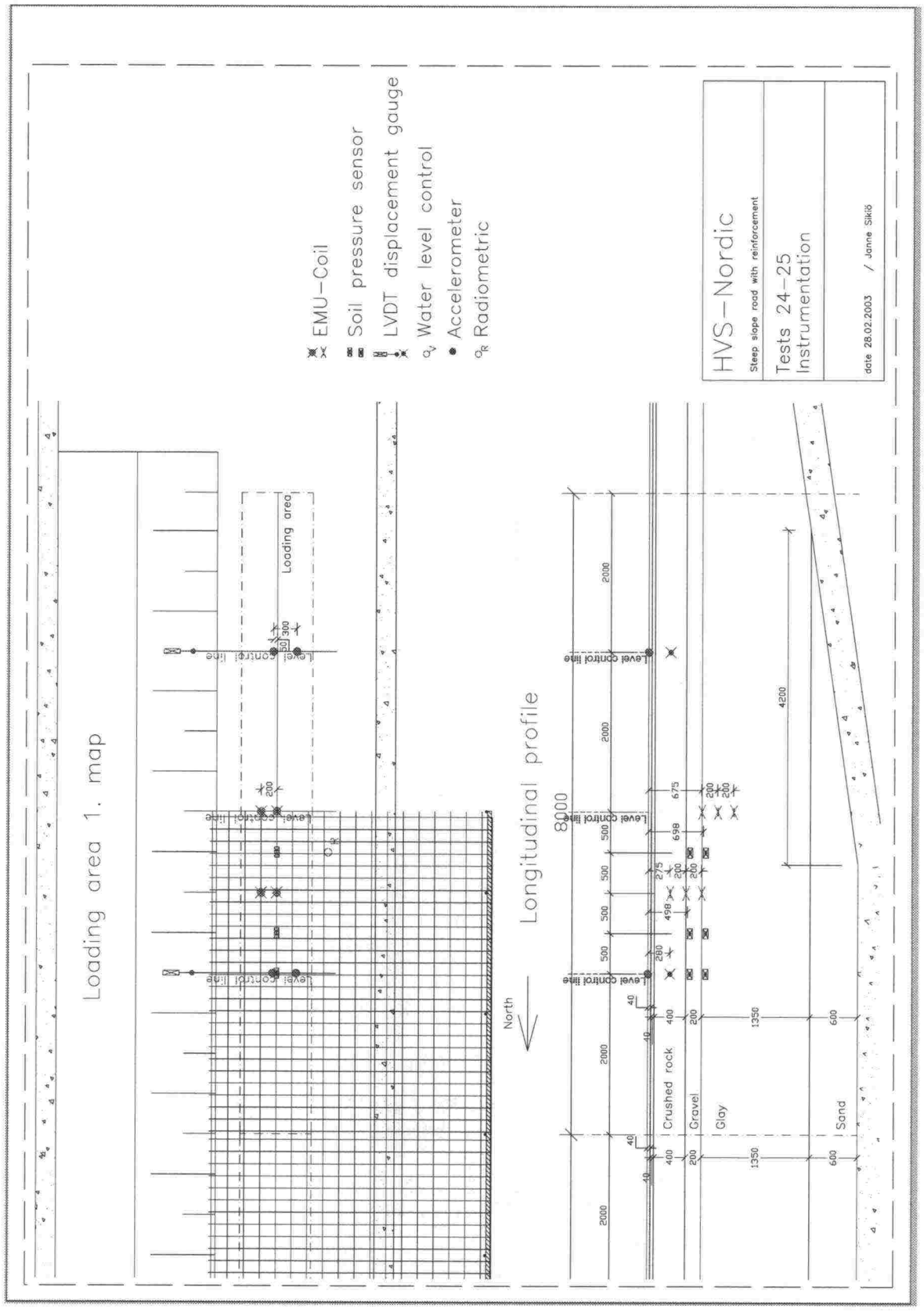
EMU-Coil
Soil pressure sensor
LVDT displacement gauge
Water level control
Accelerometer
Radiometric
HVS-Nordic
Steep slope road with reinforcement
Tests 24-25
Instrumentation
date 28.02.2003 / Janne Sikiö
Loading area 1. map
Loading area
Level control line
Longitudinal profile
North
8000
Crushed rock
Gravel
Clay
Sand
2000
4200
1350
675
698
498
280
275

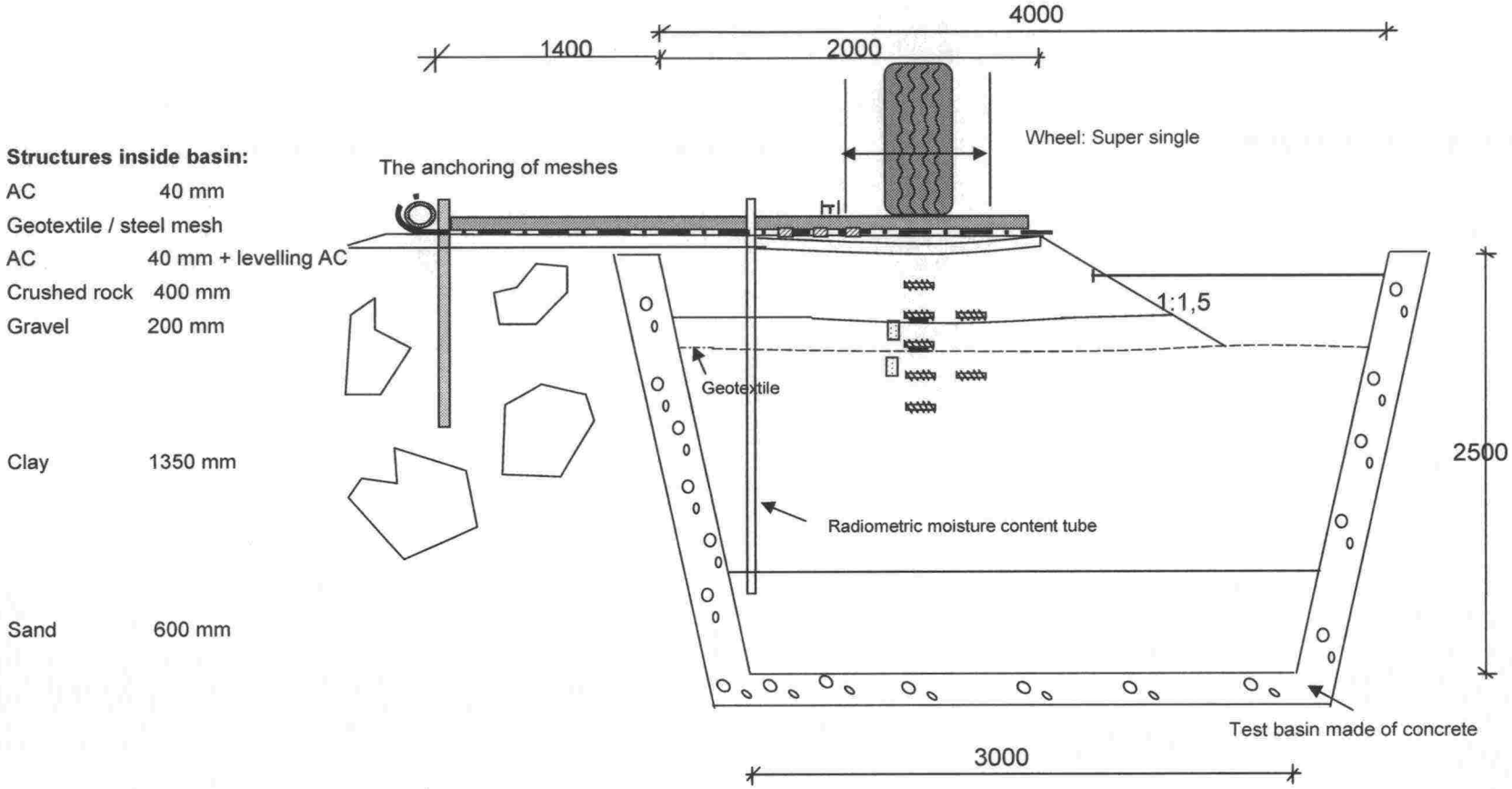

Response measurements

- = EMU coil (displacement gauge), 8 unit / section
- = Strain gauges of the mesh 2 x 3 /steel mesh
- = LVDT displacement gauge, 2 unit/section
- = Earth pressure cell, 6-10 unit / section
- = Deflection gauge (acceleration transducer), 1 unit/section
- = Pore pressure gauge, 2 unit / section

Other measurements

- FWD
- Sampling
- Radiometric measurement
- Profile (AC surface and slope)
- Temperature control
- Damage inventory
- Control measurements during construction

APPENDIX 2. QUALITY CONTROL MEASUREMENTS DURING CONSTRUCTION

(LV = Low-Volume test)

Table A2.1. Levelling results for the upper surface of asphalt layer.

Before rehabilitation	**Str24-25**	**Str26-27**	**Str28-29**	**Date**
Average	+16.37	+16.34	+16.35	3.9.2002
Deviation	15.2	11.9	7.9	
Min	+16.35	+16.33	+16.34	
Max	+16.40	+16.36	+16.37	
After levelling mass	**Str 24-25**	**Str 26-27**	**Str 28-29**	**Date**
Average	+16.40	+16.38	+16.40	5.9.2002
Deviation	6.8	7.6	3.9	
Min	+16.38	+16.37	+16.39	
Max	+16.41	+16.40	+16.40	
After rehabilitation	**Str 24-25**	**Str 26-27**	**Str 28-29**	**Date**
Average	+16.43	+16.42	+16.44	26.9.2002
Deviation	4.9	7.5	5.0	
Min	+16.43	+16.42	+16.43	
Max	+16.44	+16.44	+16.44	

Table A2.2. The average thickness (mm) of the asphalt layers and their deviations on the loading area. The values do not consider to the possible changes of the thickness of the LV asphalt layer during the first loading phase.

Thickness / deviation. mm	**Str 24-25**	**Str 26-27**	**Str 28-29**
LV asphalt layer	42.57 / 4.8	37.71 / 2.6	41.43 / 4.2
Levelling mass	36.71 / 8.0	48.14 / 4.2	48.57 / 5.5
New asphalt layer	36.29 / 6.9	39.29 / 7.2	38.71 / 8.5

Table A2.3. The bearing measurements during the construction phase. E_2 is converted to the temperature of +20 °C.

Bearing capasity E_2. MPa (+20° C)	**Before LV-test. W1**	**Estimated after LV-test**	**On levelling mass W2**	**Rehabilitated W2**
Str 24-25	91	82	127	209
Str 26-27	81	49	132	216
Str 28-29	83	41	128	206
Date	9.7.2001	Autumn 2001	18.9.2002	24.9.2002

APPENDIX 3. RADIOMETRIC MEASUREMENTS

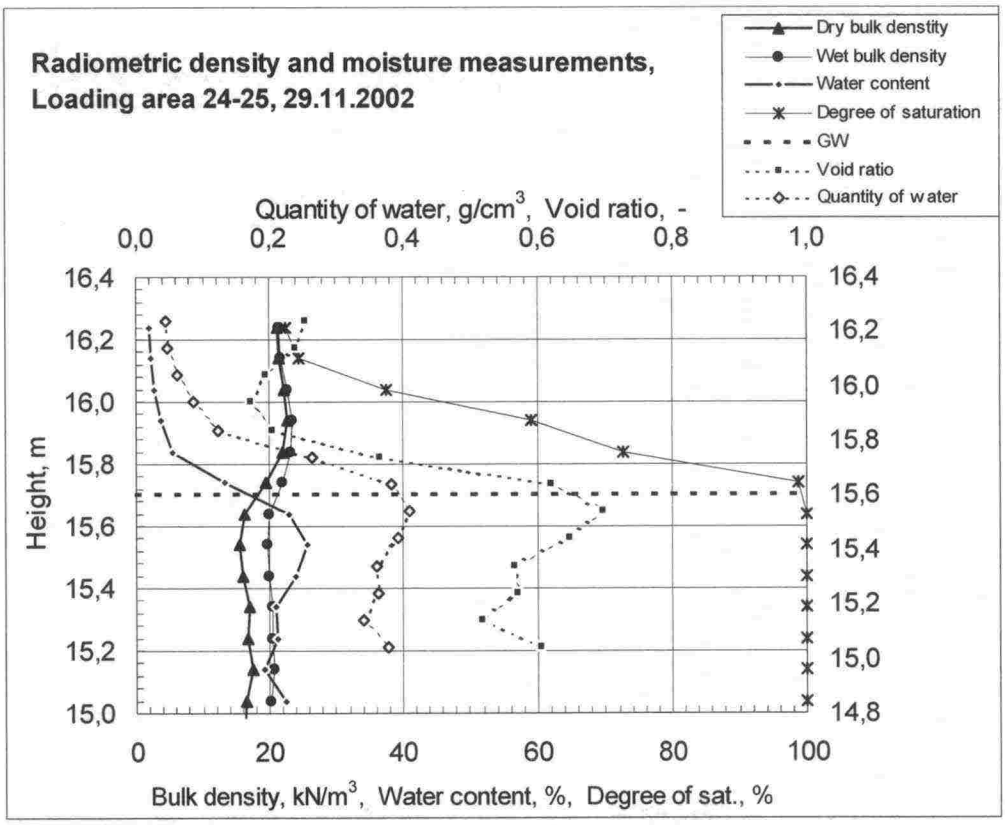

Figure L3.1. Structure 24 -25. Radiometric measurements before test W1.

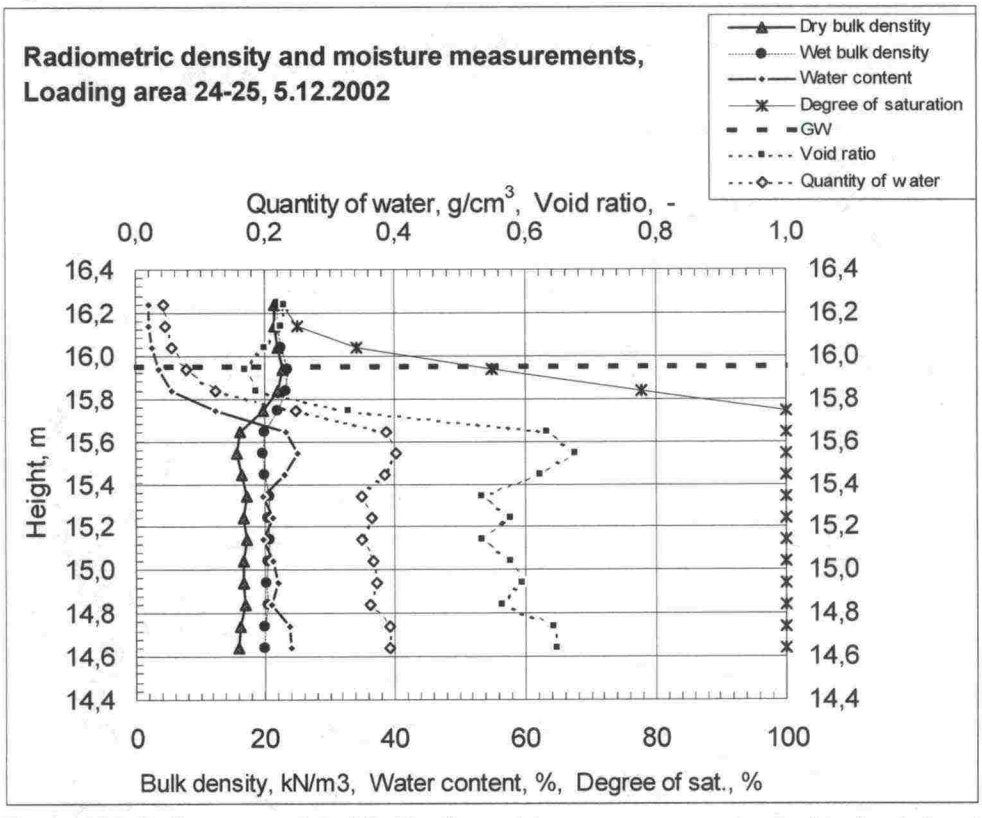

Figure A3.2. Structure 24 -25. Radiometric measurements during test, level W2.

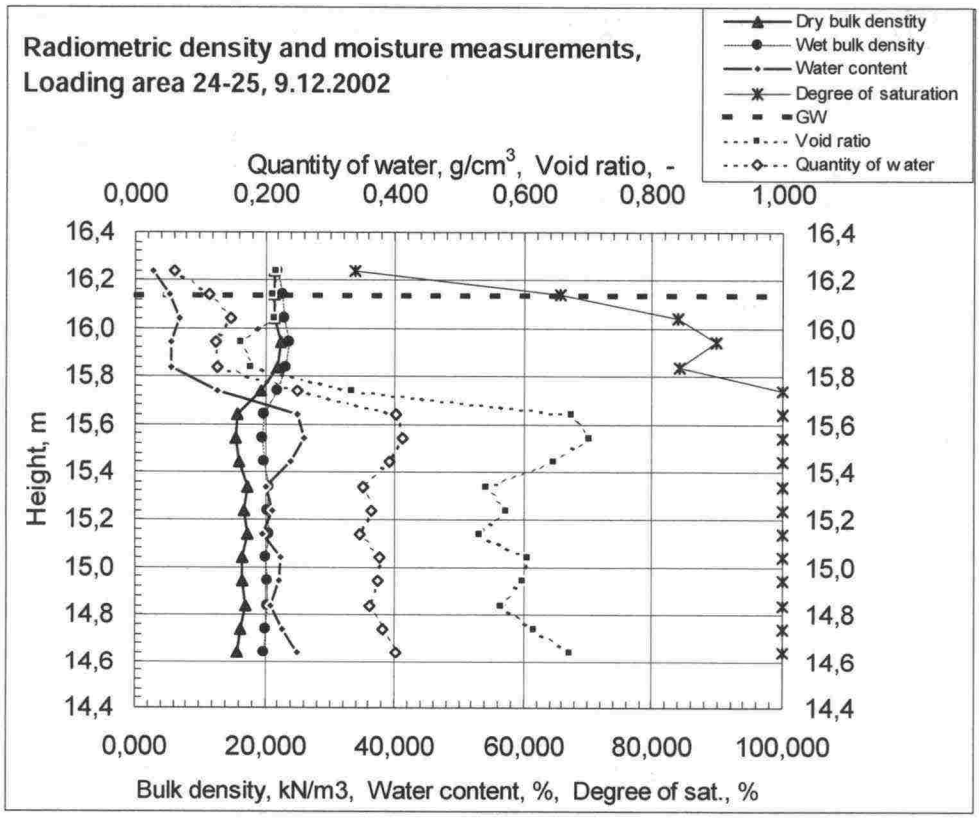

Figure A3.3. Structure 24 -25. Radiometric measurements during the test level W3.

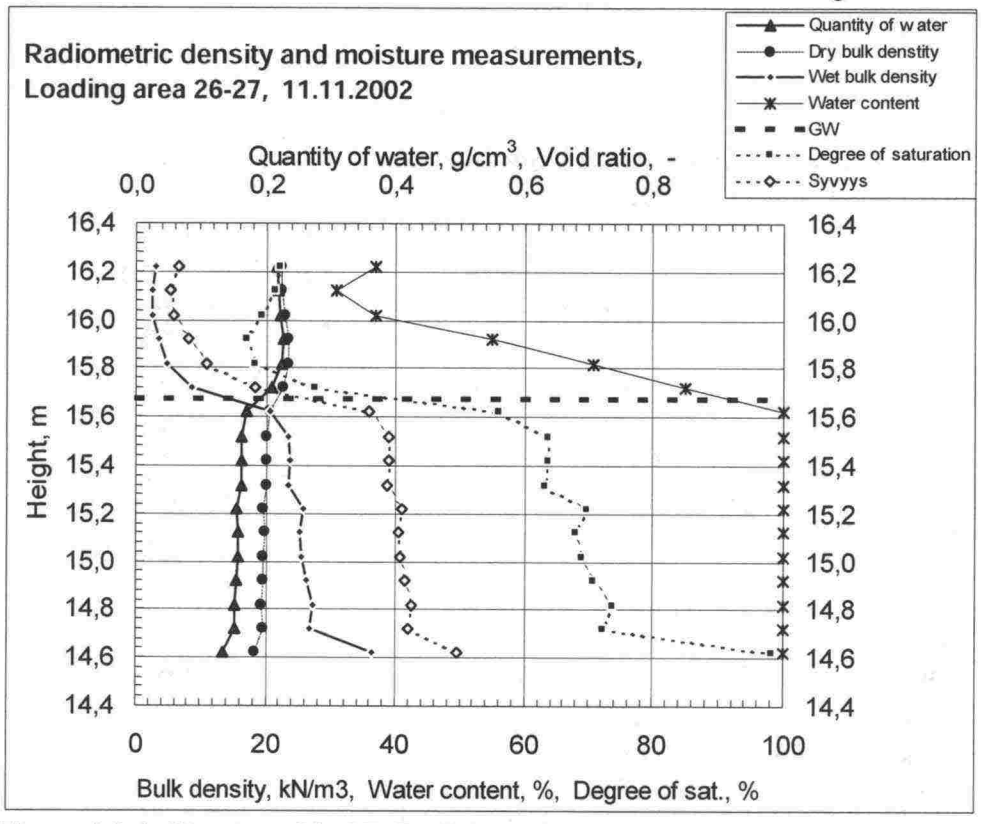

Figure A3.4. Structure 26 -27. Radiometric mesurements before test W1.

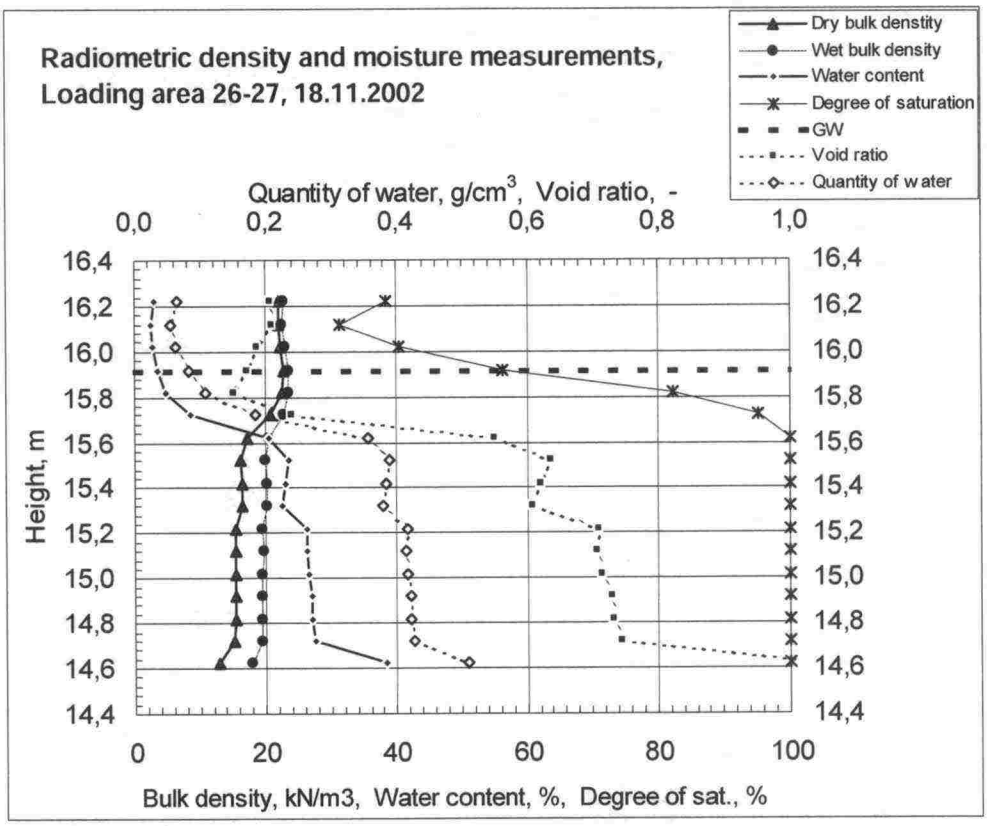

Figure A3.5. Structure 26 -27. Radiometric measurements during test level W2.

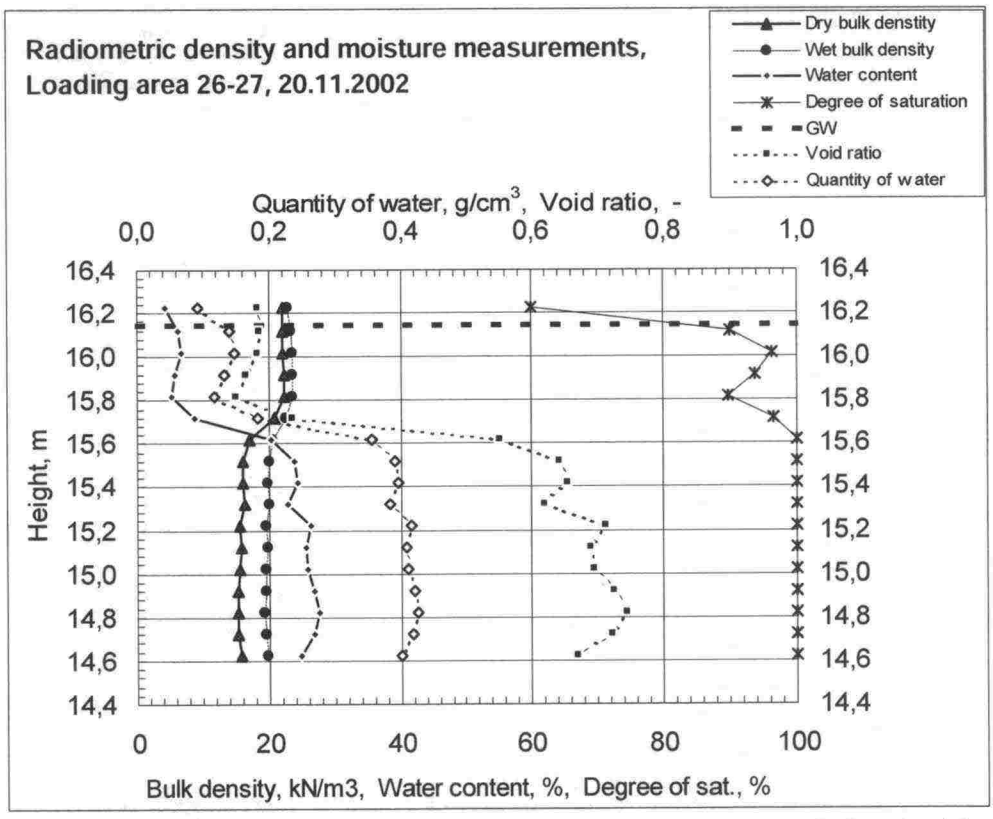

Figure A3.6. Structure 26 -27. Radiometric measurements during test level W3.

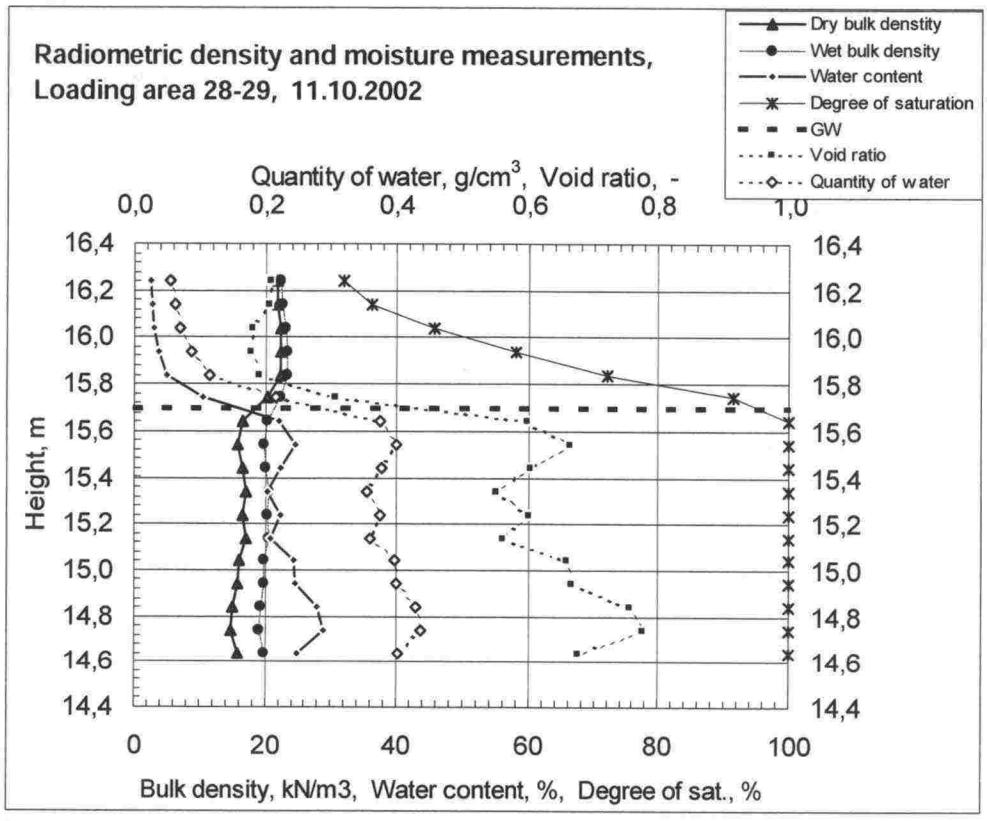

Figure A3.7. Structure 28 -29. Radiometric mesurements before test W1.

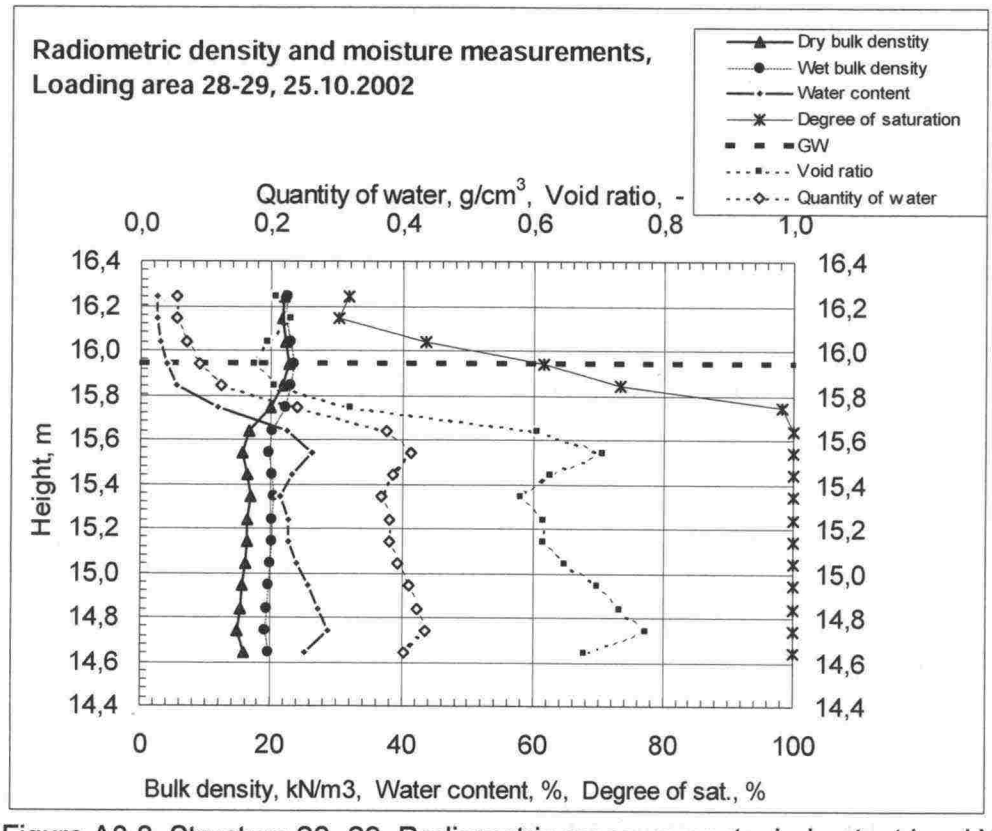

Figure A3.8. Structure 28 -29. Radiometric measurements during test level W2.

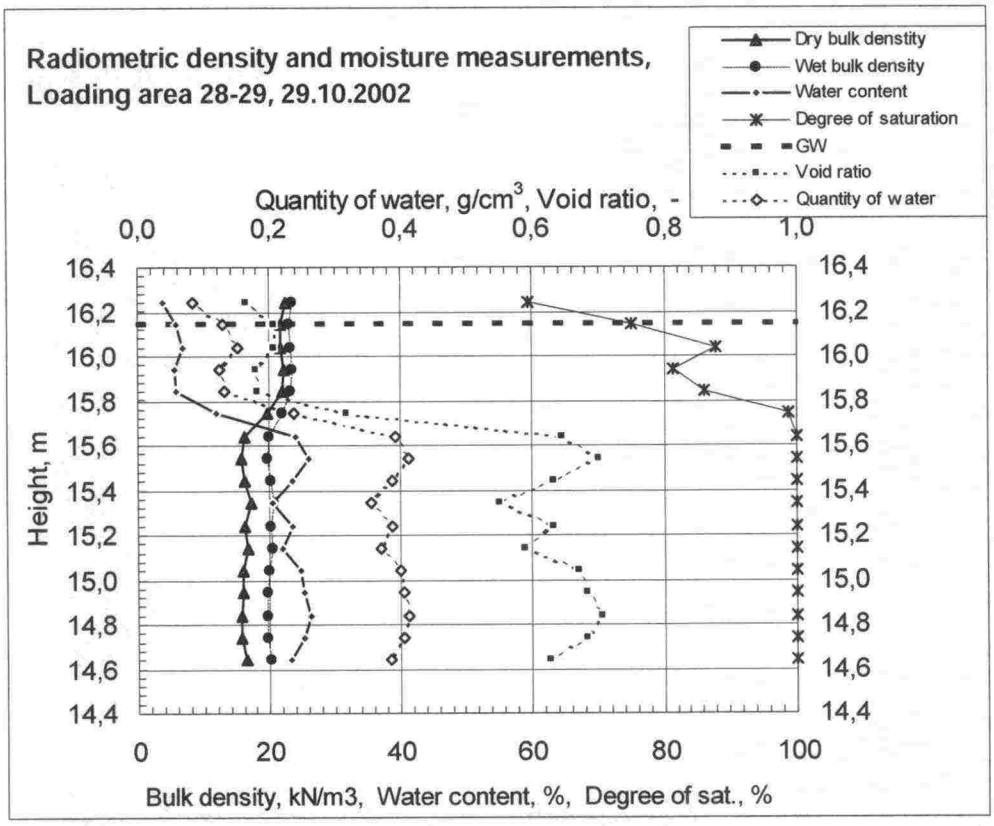

Figure A3.9. Structure 28 -29. Radiometric measurements during test level W3.

APPENDIX 4. EARTH PRESSURE MEASUREMENTS

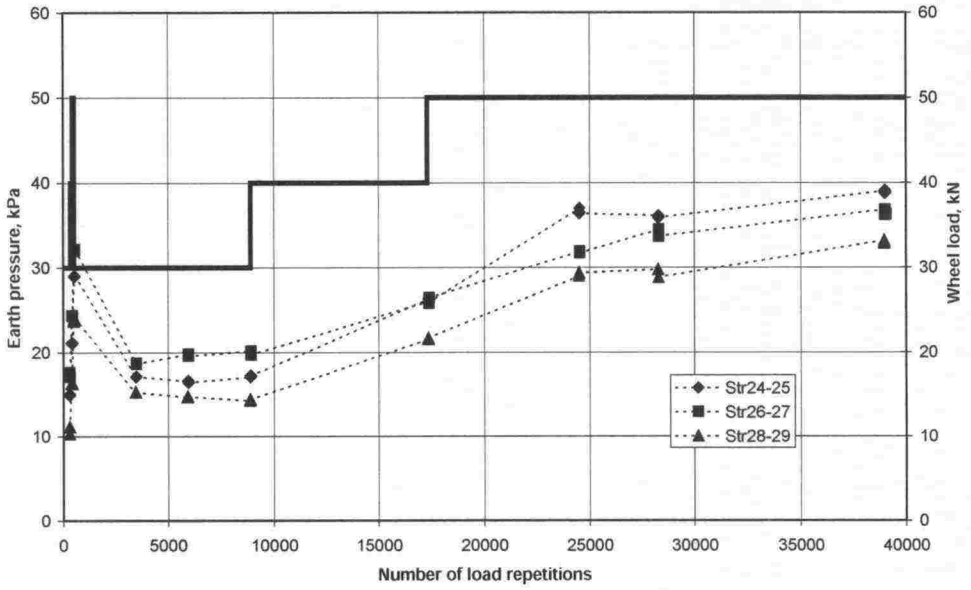

Figure A4.1. The transient earth pressure in the upper part of the clay in different structures. All earth pressure cells of the structure 24-25 have been situated in the structure 25 and respectively in the structure 28 ot the structure pair 28-29. In structure pair 26-27 two earth pressure cells have been situated in structure 26 and one in structure 27.

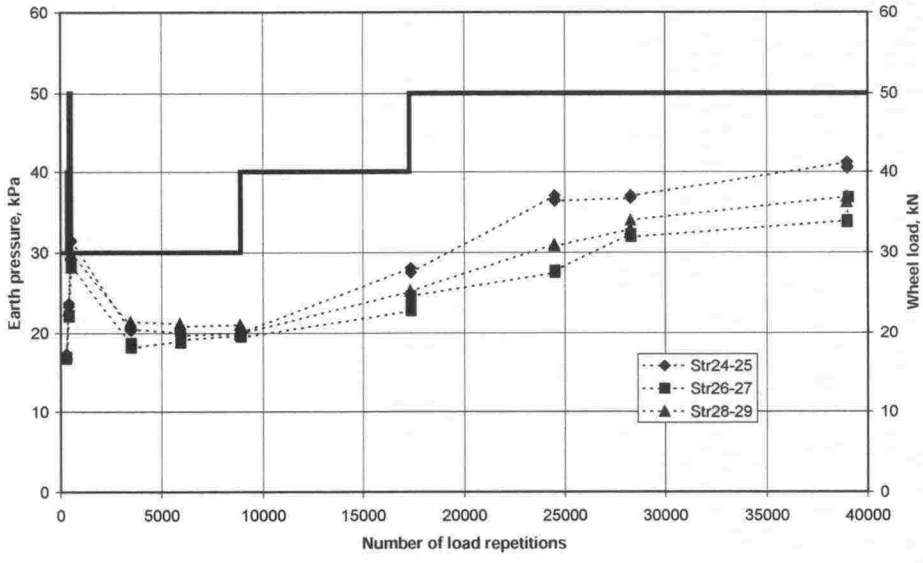

Figure A4.2. The transient earth pressure in the gravel in different structures. All earth pressure cells of the structure 24-25 have been situated in the structure 25 and respectively in the structure 28 ot the structure pair 28-29. In structure pair 26-27 two earth pressure cells have been situated in structure 26 and one in structure 27.

APPENDIX 5. DEFORMATION MEASUREMENTS

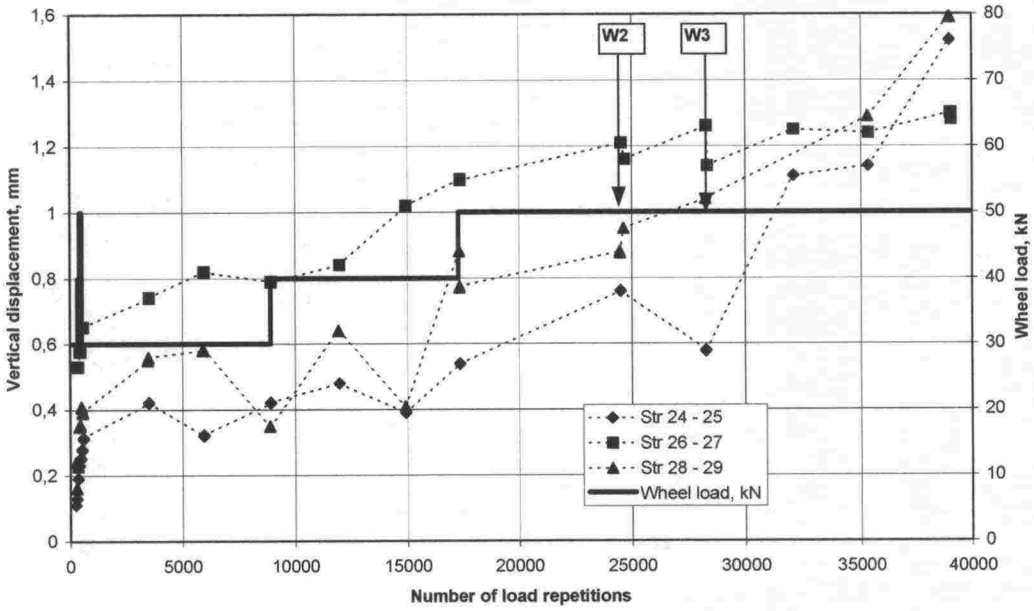

Figure A5.1. The permanent vertical displacement of the lower part of the crushed rock.

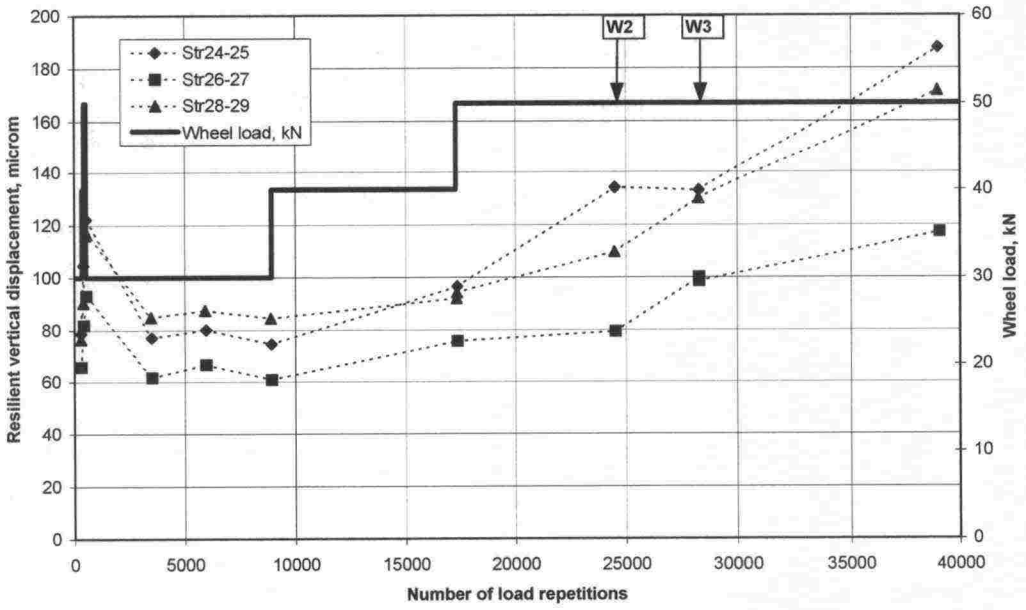

Figure A5.2. The resilient vertical displacement of the lower part of the crushed rock.

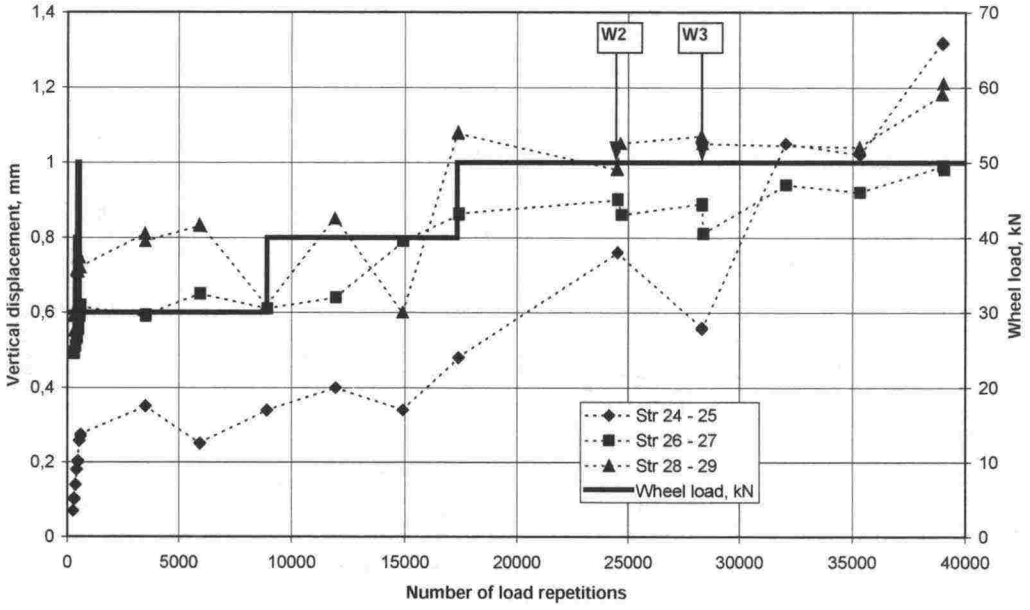

Figure A5.3. The permanent vertical displacement of the lower part of the gravel.

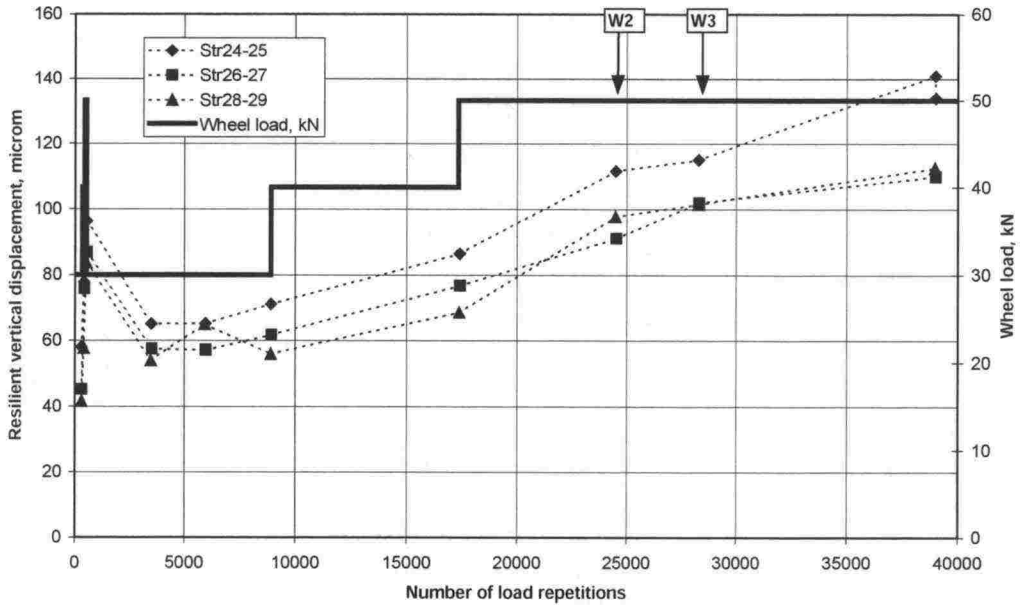

Figure A5.4. The resilient vertical displacement of the lower part of the gravel.

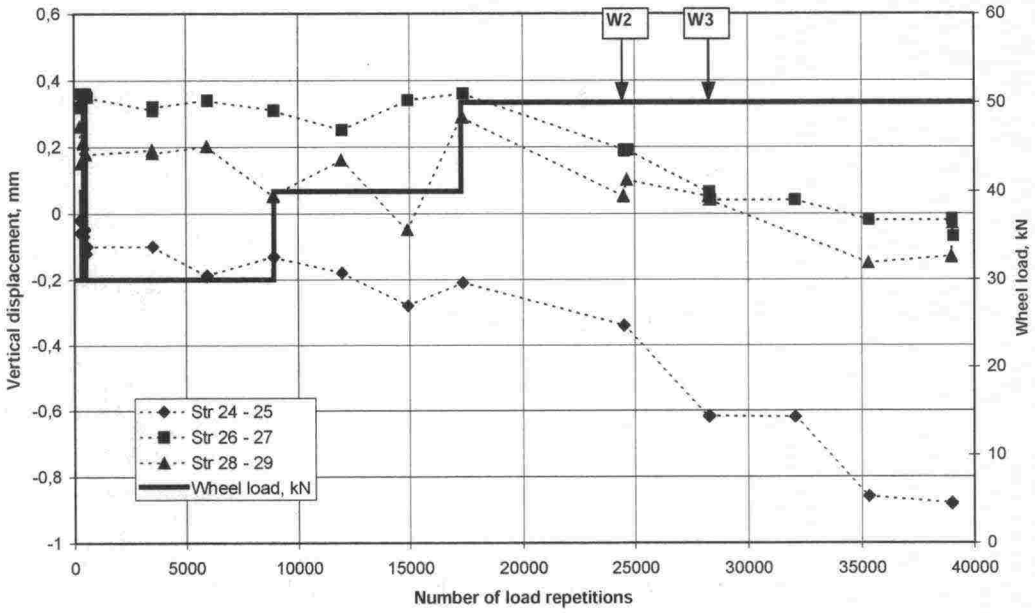

Kuva A5.5. The permanent horizontal displacement of the interface of the gravel annd crushed rock.

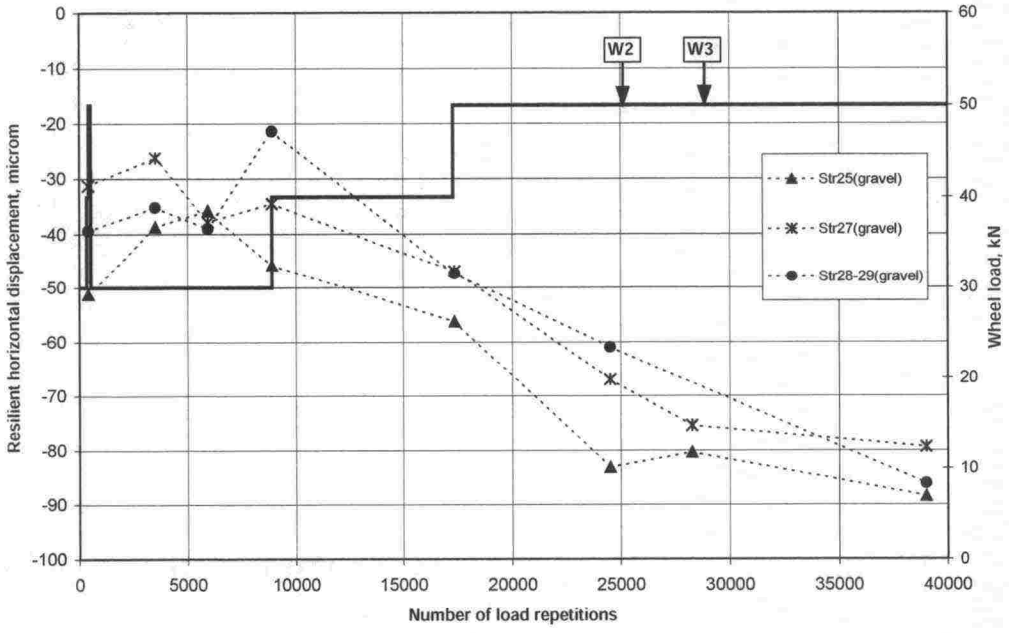

Figure A5.6. The resilient horizontal displacement of the interface of the gravel annd crushed rock.

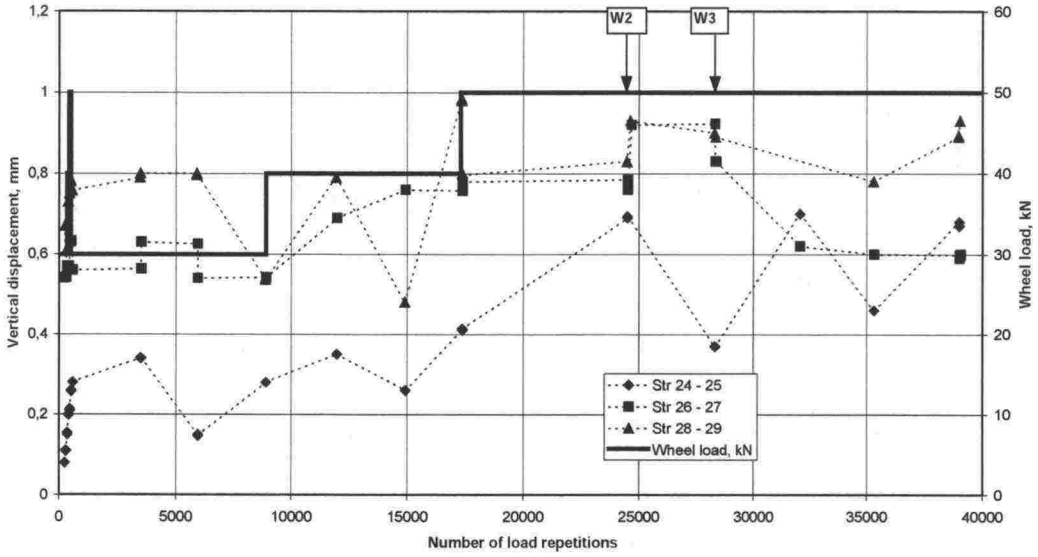

Figure A5.7. The permanent vertical displacement of the upper part of the clay (0-200mm).

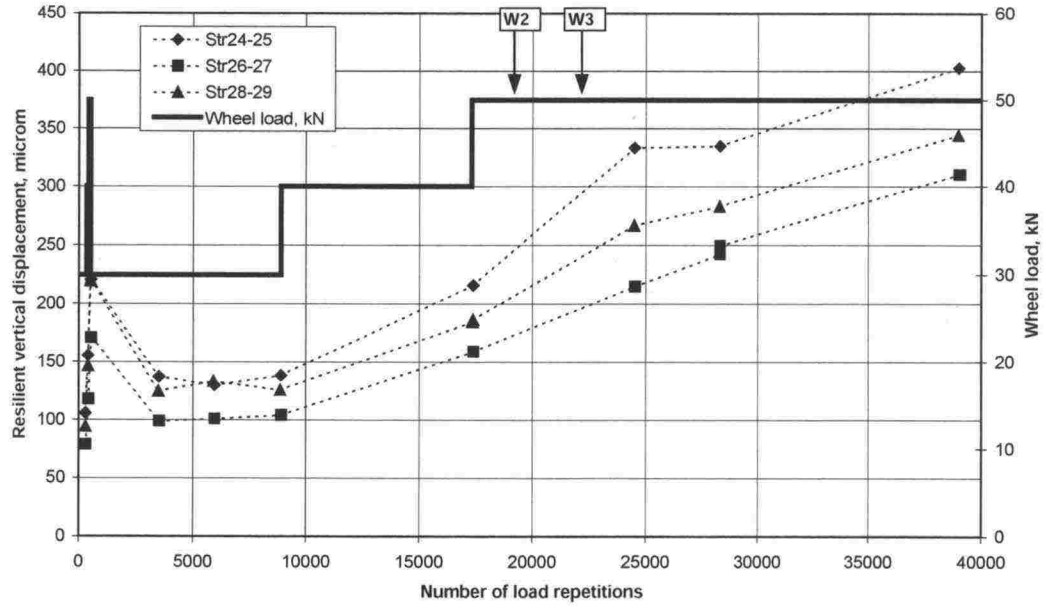

Figure A5.8. The resilient vertical displacement of the upper part of the clay (0-200mm).

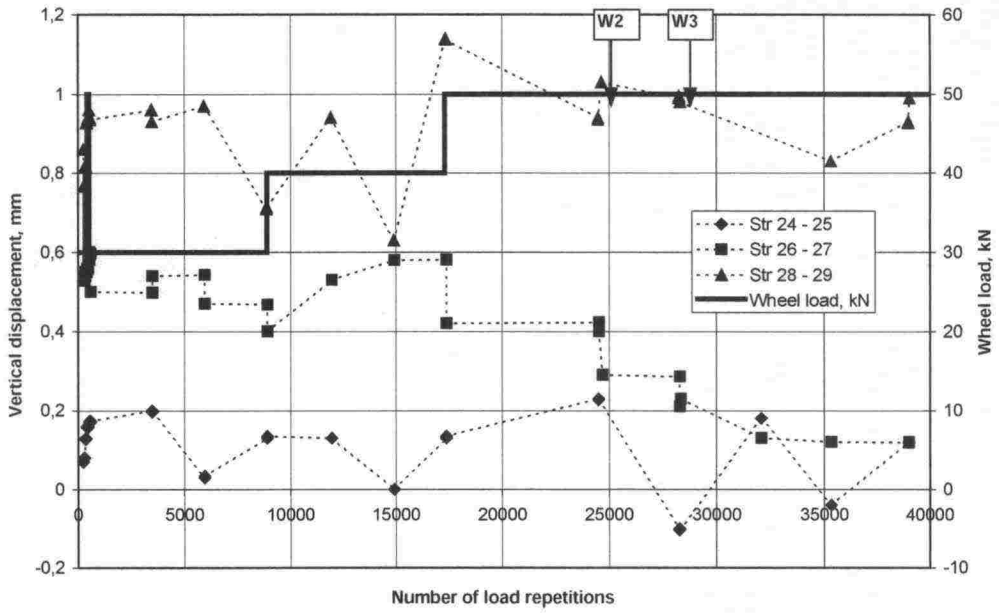

Figure A5.9. The permanent vertical displacement of the lower part of the clay (200-400mm).

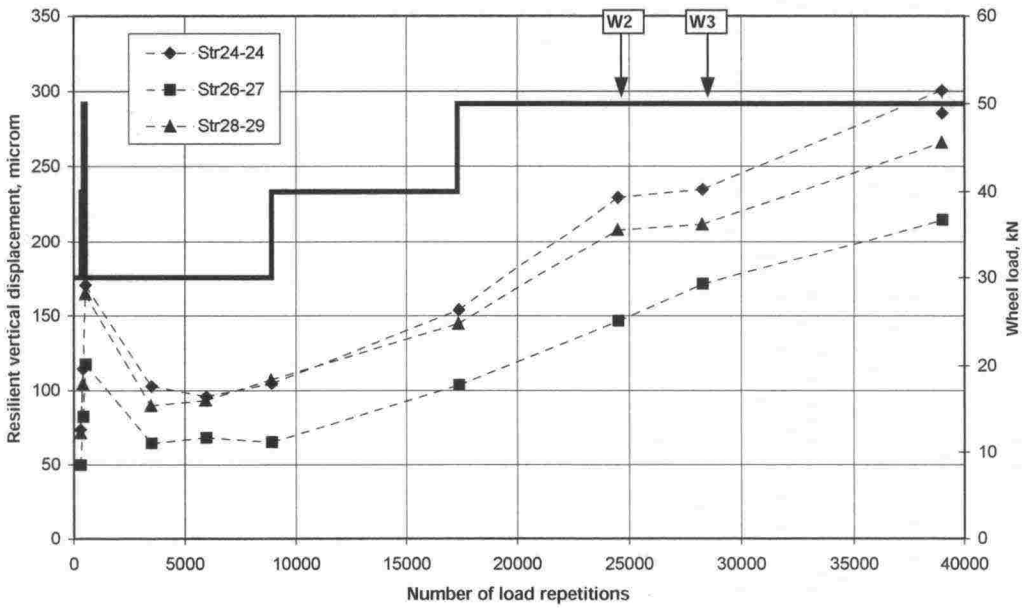

Figure A5.10. The resilient vertical displacement of the lower part of the clay (200-400mm).

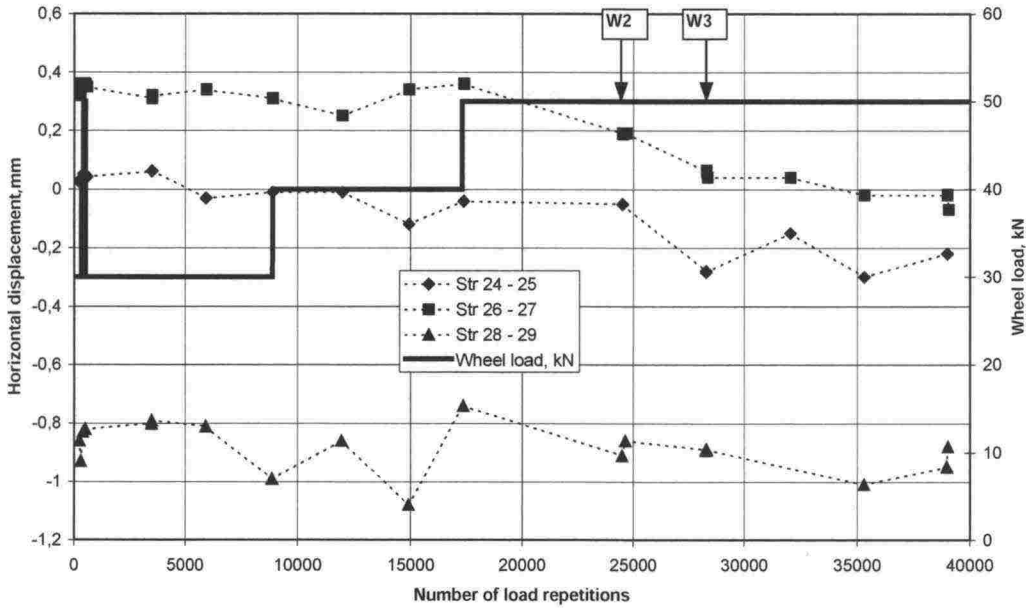

Figure A5.11. The permanent horizontal displacement of the interface of the clay in depth 200 mm.

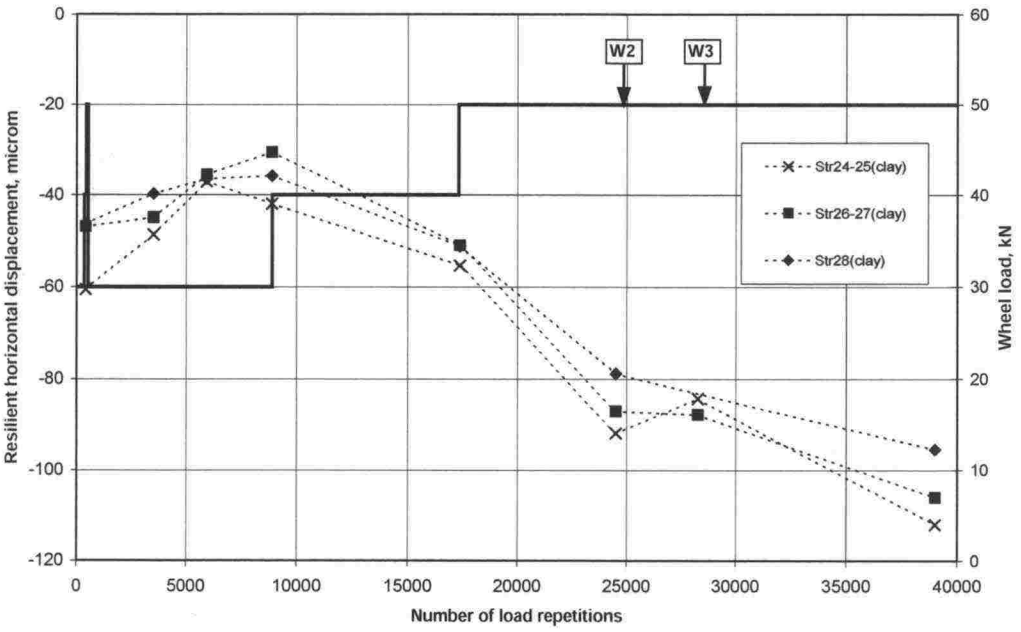

Figure A5.12. The resilient horizontal displacement of the interface of the clay in depth 200 mm.

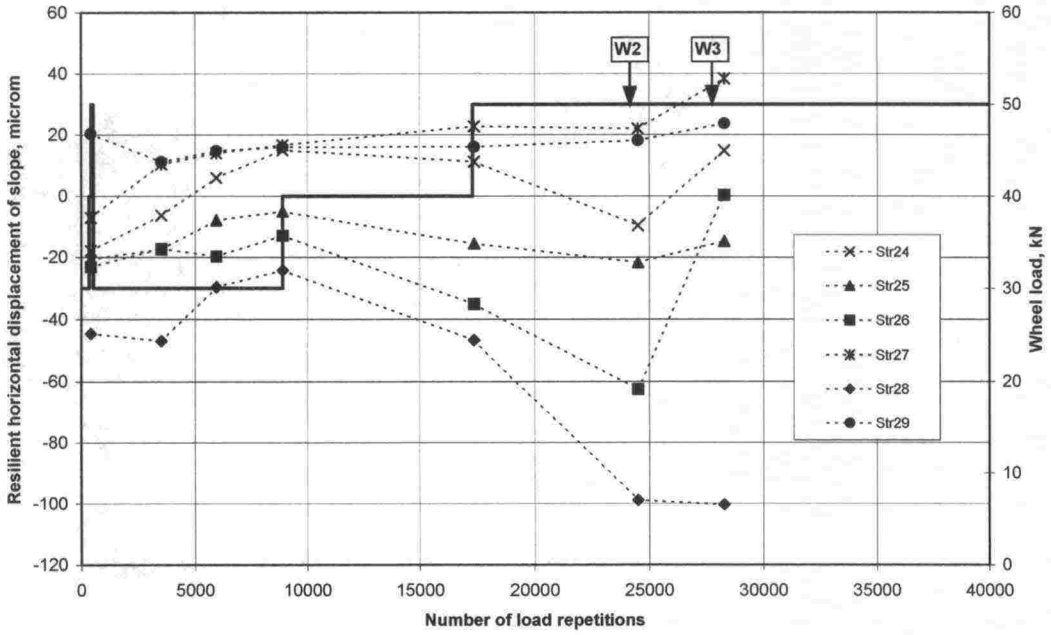

Figure A5.13. The resilient displacement of the slope in different structures. The negative value is for the pavement's displacement towards the slope.

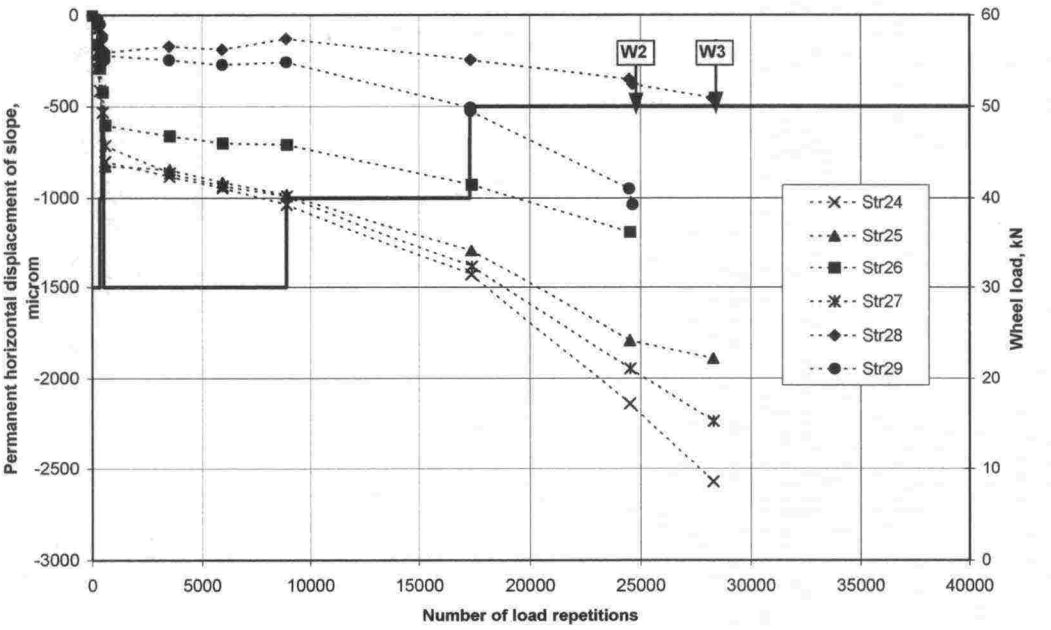

Figure A5.14. The permanent displacement of the slope in differenr structures. The negative value is for the pavement's displacement towards the slope.

APPENCIX 6. PROFILOMETER MEASUREMENTS

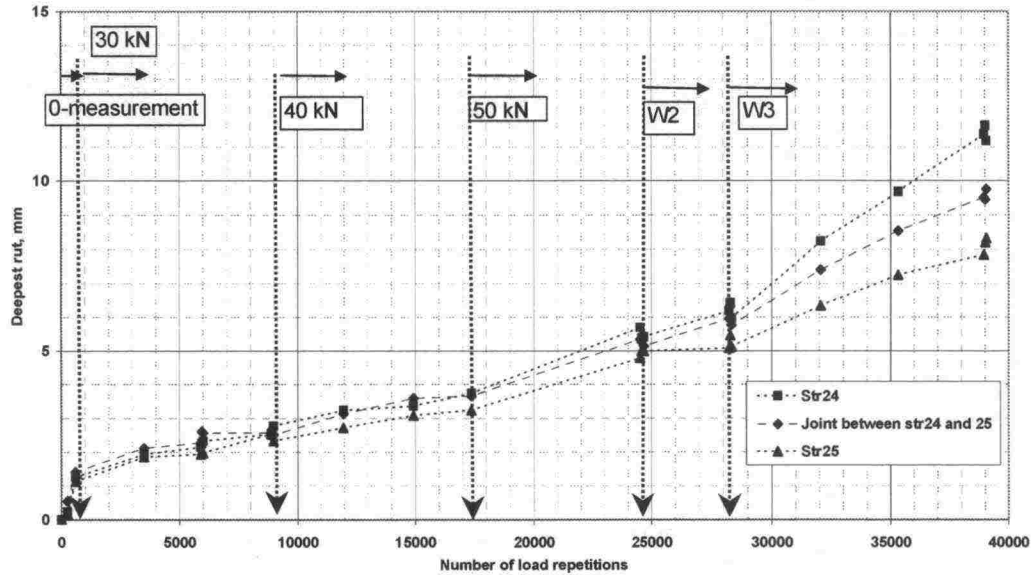

Figure A6.1. Average depth of the rut according to the profilometer measurements of the structure 24 - 25 in the deepest part of the rut.

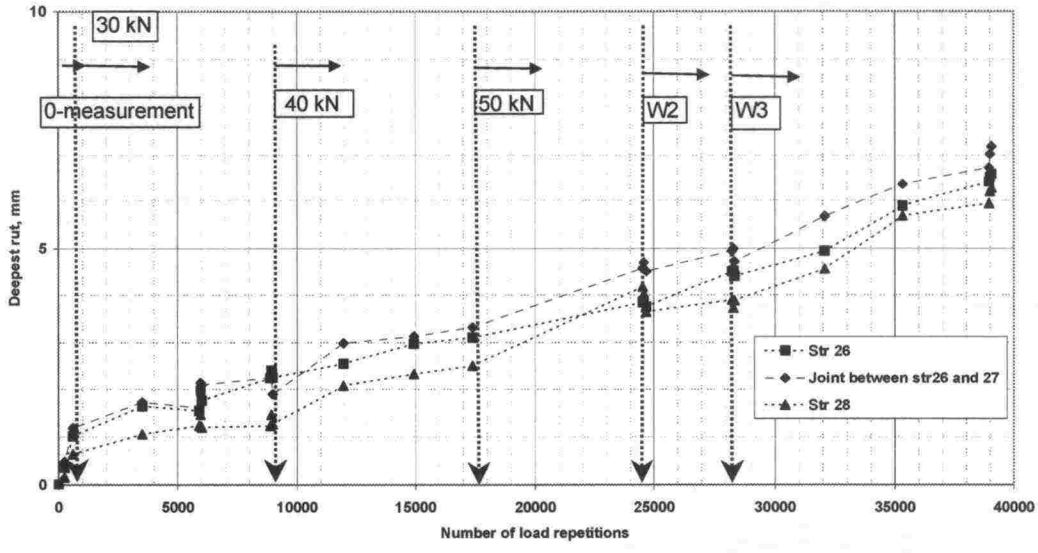

Figure A6.2. Average depth of the rut according to the profilometer measurements of the structure 26 - 27 in the deepest part of the rut.

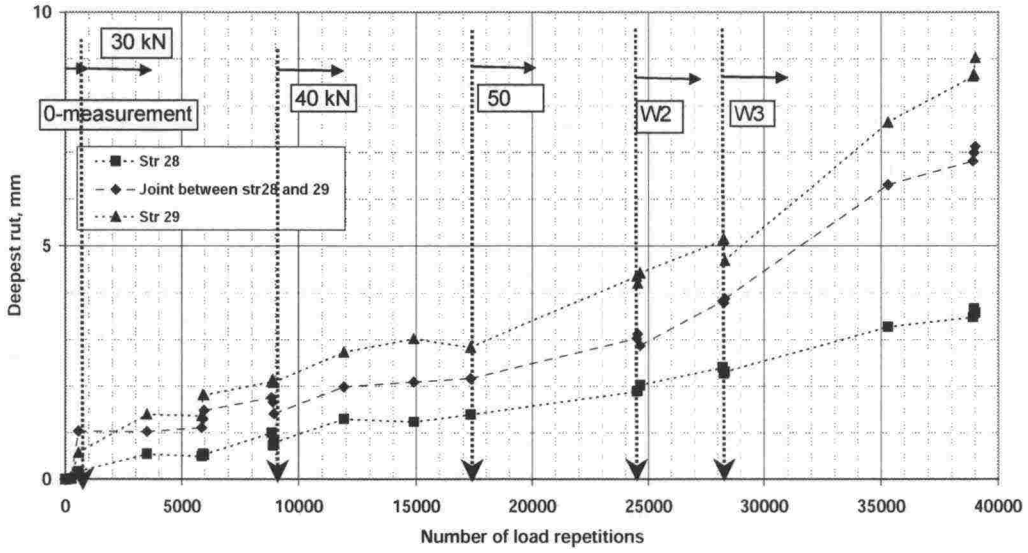

Figure A6.3. Average depth of the rut according to the profilometer measurements of the structure 28 - 29 in the deepest part of the rut.

APPENDIX 7. STRAIN MEASUREMENTS OF REINFORCEMENTS

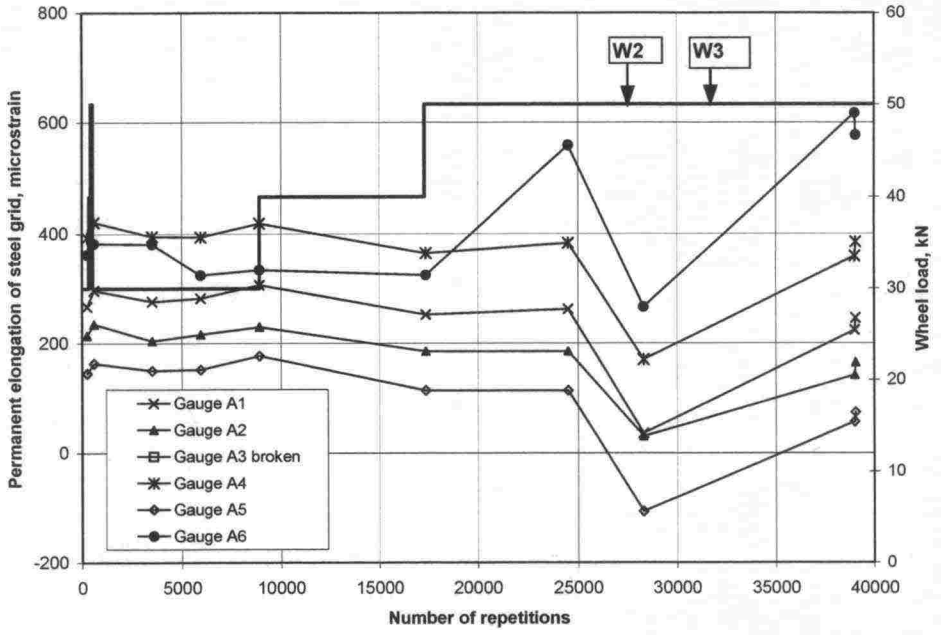

Figure A7.1. The permanent elongation in the steel grid in structure 25.

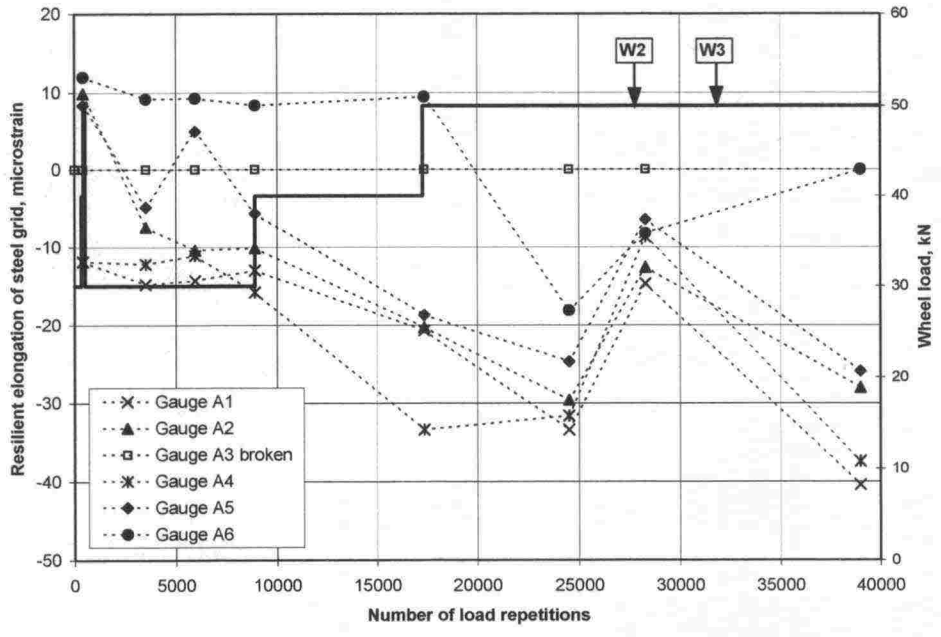

Figure A7.2. The resilient elongation in the steel grid in structure 25.

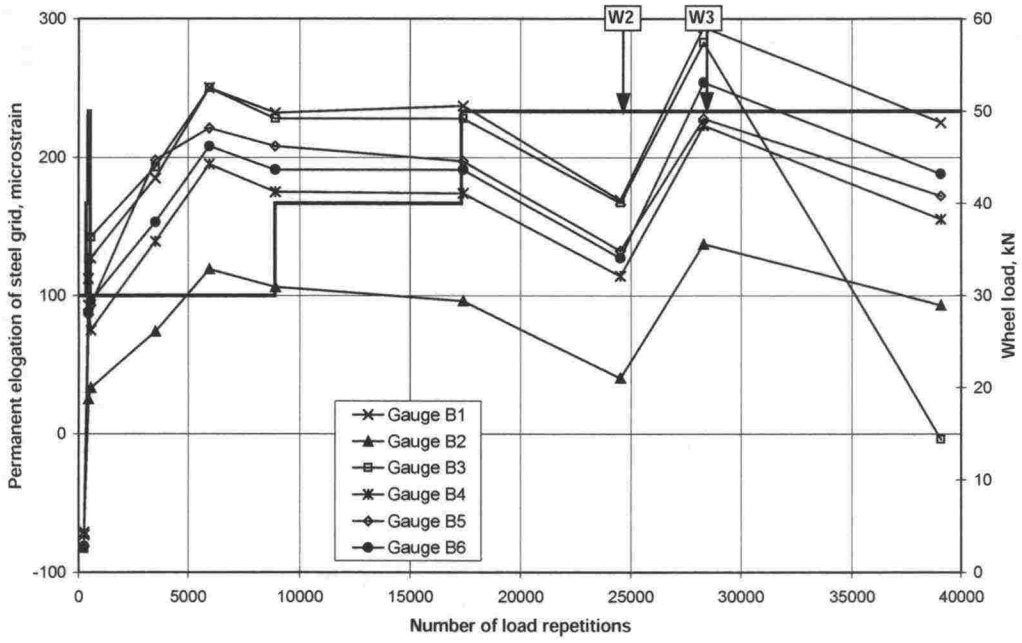

Figure A7.3. The permanent elongation in the steel grid in structure 26.

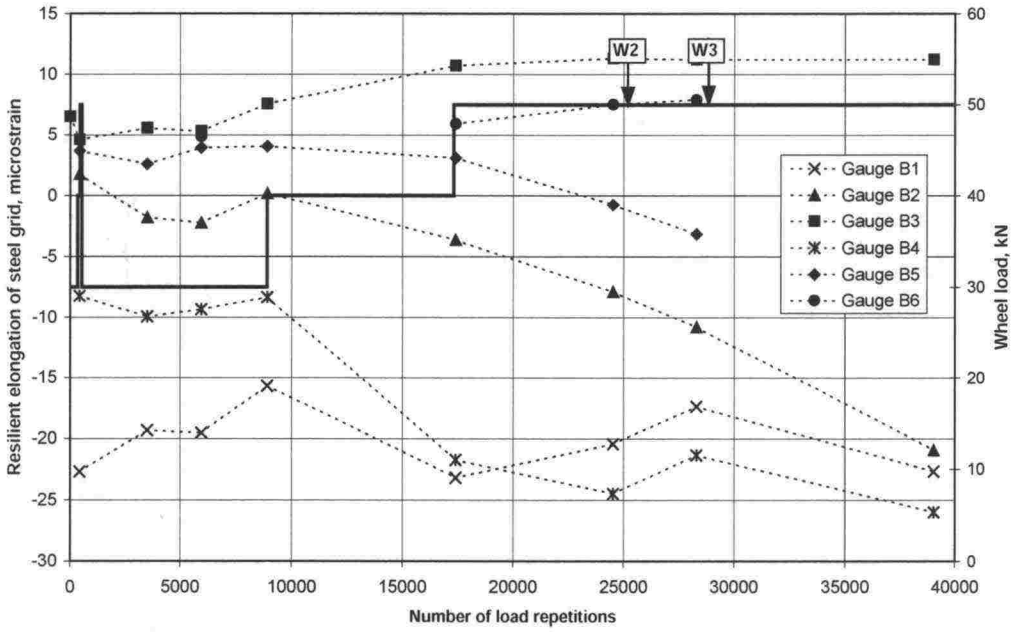

Figure A7.4. The resilient elongation of the steel grid in structure 26.

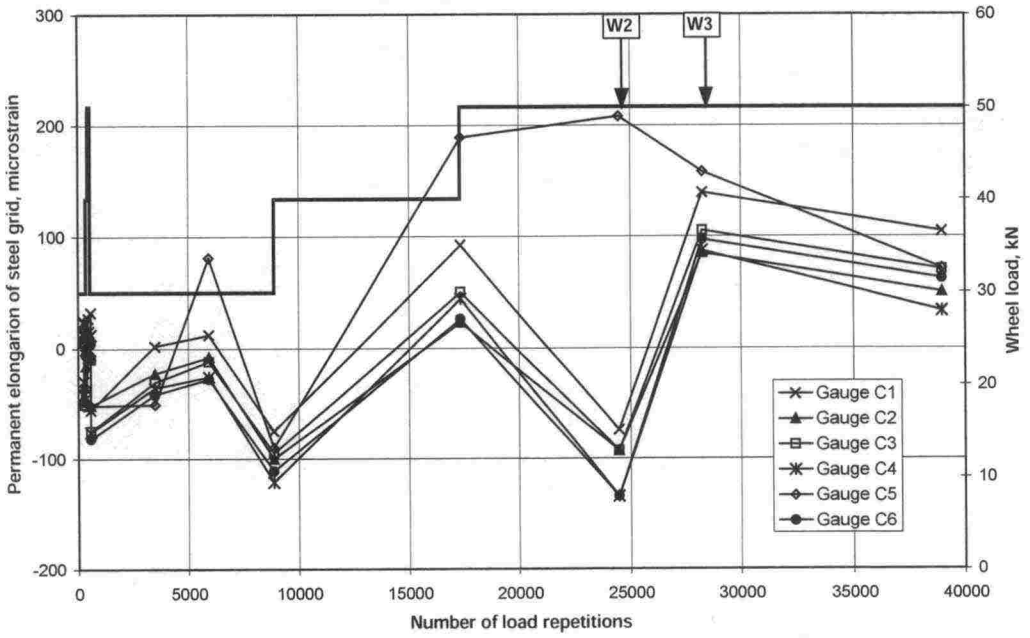

Figure A7.5. The permanent elongation in the steel grid in structure 28.

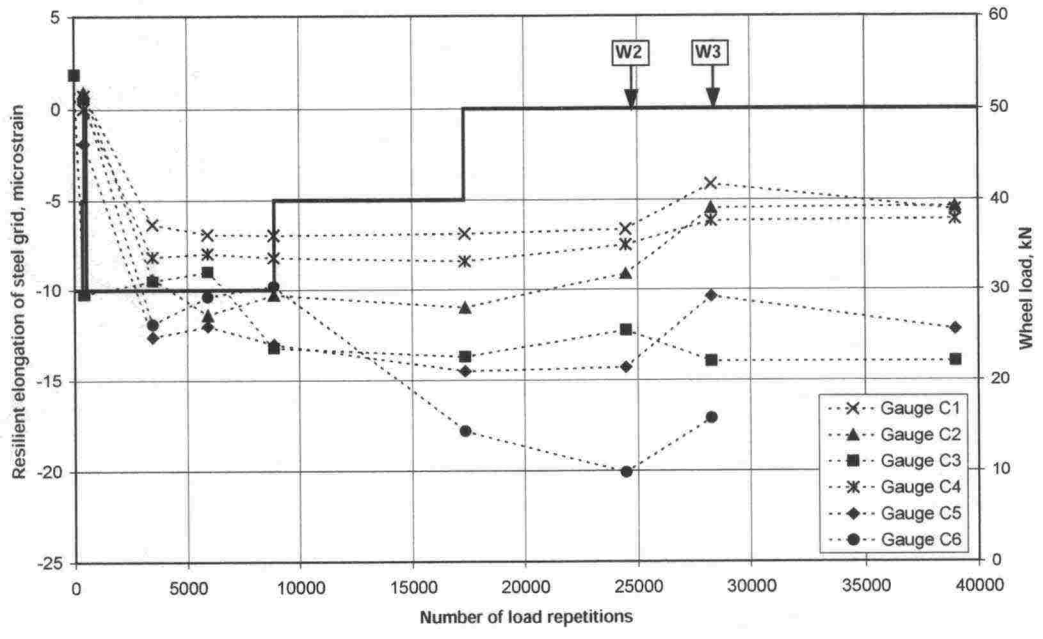

Figure A7.6. The resilient elongation of the steel grid in structure 28.

ISSN 1457-9871
ISBN 951-803-107-x
TIEH 3200825E